The Rhizobial effector NopT targets Nod factor receptors to regulate symbiosis in *Lotus japonicus*

Hanbin Bao[1#], Yanan Wang[1#], Haoxing Li[1], Qiang Wang[1], Yutao Lei[1], Ying Ye[1], Syed F. Wadood[2], Hui Zhu[1], Christian Stahelin[2], Gary Stacey[3], Shutong Xu[1], Yangrong Cao[1*]

[1] National Key Lab of Agricultural Microbiology, Hubei Hongshan Laboratory, Huazhong Agricultural University, Wuhan, Hubei, 430070, China

[2] State Key Laboratory of Biocontrol and Guangdong Key Laboratory of Plant Resources, School of Life Sciences, Sun Yat-sen University, Guangzhou, 510275, China

[3] Divisions of Plant Science and Technology and Biochemistry, Christopher S. Bond Life Sciences Center, University of Missouri, Columbia, MO 65211, USA

# These authors contributed equally to this work.

* Corresponding author: Yangrong Cao, email: yrcao@mail.hzau.edu.cn

Short title: NopT associates with NFR1 and NFR5 to regulate symbiosis

Keywords: Legume-rhizobium symbiosis; Rhizobial effector; Nod factor receptors; NopT.

One-sentence summary: The rhizobial effector NopT and two Nod factor receptors of *Lotus japonicus*, NFR1 and NFR5, mutually interact to precisely regulate rhizobial symbiosis.

Abstract

It is well-documented that type-III effectors are required by Gram-negative pathogens to directly target different host cellular pathways to promote bacterial infection. However, in the context of legume-rhizobium symbiosis, the role of rhizobial effectors in regulating plant symbiotic pathways remains largely unexplored. Here, we show that NopT, a YopT-type cysteine protease of *Sinorhizobium fredii* NGR234 directly targets the plant's symbiotic signaling pathway by associating with two Nod factor receptors (NFR1 and NFR5 of *Lotus japonicus*). NopT inhibits cell death triggered by co-expression of NFR1/NFR5 in *Nicotiana benthamiana*. Full-length NopT physically interacts with NFR1 and NFR5. NopT proteolytically cleaves NFR5 both *in vitro* and *in vivo*, but can be inactivated by NFR1 as a result of phosphorylation. NopT plays an essential role in mediating rhizobial infection in *L. japonicus*. Autocleaved NopT retains the ability to cleave NFR5 but no longer interacts with NFR1. Interestingly, genomes of certain *Sinorhizobium* species only harbor *nopT* genes encoding truncated proteins without the autocleavage site. These results reveal an intricate interplay between rhizobia and legumes, in which a rhizobial effector protease targets NFR5 to dampen symbiotic signaling. NFR1 appears to counteract this process by phosphorylating the effector. This discovery highlights the role of a bacterial effector in regulating a signaling pathway in plants and opens up the perspective of developing kinase-interacting proteases to fine-tune cellular signaling processes in general.

Introduction

The legume–rhizobium symbiosis stands as one of the most crucial and intricate mutualistic interactions in nature. Its significance goes beyond the supply of nitrogen fixed by rhizobia, which influences plant growth and ecosystem sustainability, as this symbiosis is a pivotal model for investigating plant-microbe interactions (Yang et al., 2022). The orchestration of this symbiosis involves the perception of rhizobial signal molecules such as lipo–chitooligosaccharidic Nod factors (NFs) and surface

polysaccharides (Madsen et al., 2003; Tirichine et al., 2006; Kawaharada et al., 2015), along with the secretion of proteins, including type three protein secretion system (T3SS) effectors translocated into host plants (Sugawara et al., 2018; Zhang et al., 2021).

Plant receptor heterocomplexes consisting of two Lysin-motif receptor kinases (LYKs), play a central role in recognizing various microbial poly- and oligosaccharide molecules. In non–legumes such as Arabidopsis, AtLYK5 and AtCERK1 (Chitin elicitor receptor kinase) are required for perception of chitin, and thereby trigger plant immunity to combat fungal pathogens (Cao et al., 2014). In legumes, structurally similar Nod factor receptors (NFRs) such as NFR1 and NFR5 in *Lotus japonicus* are vital for recognition of rhizobial NFs and initiation of symbiotic signaling (Broghammer et al., 2012; Bozsoki et al., 2017). Accordingly, *nfr1* and *nfr5* knockout mutants are almost completely unable to form nodules (Madsen et al., 2003; Radutoiu et al., 2003). Over-expression of either NFR1 or NFR5 can activate NF signaling, resulting in formation of spontaneous nodules in the absence of rhizobia (Ried et al., 2014). The intricate action of NFRs is highlighted by the elictiation of a hypersensitive cell death response when NFR1/NFR5 are simultaneous over-expressed in *Nicotiana benthamiana* leaves (Madsen et al., 2011). Similarly, defense-like responses in *Medicago truncatula* nodules were observed upon over–expression of MtNFP (Nod factor perception, the ortholog of NFR5) (Moling et al., 2014), perhaps reflecting a potential role of MtNFP–interacting LYKs involved in plant–pathogen associations. It can therefore be expected that the protein abundance of NFRs must be tightly controlled to avoid resistance responses, thereby ensuring optimal root infection by rhizobia.

T3SS effectors of phytopathogenic Gram–negative bacteria play a critical role in suppressing pattern-triggered immunity (PTI) in host plants (Jones and Dangl, 2006). To avoid diseases, specific resistance (R) genes are employed to directly or indirectly recognize effectors translocated into host cells.

Recognition of such avirulence (Avr) effectors often results in effector-triggered immunity (ETI), a much stronger immune response which is usually associated with programmed cell death (Jones and Dangl, 2006). In contrast to the well–studied effector functions of phytopathogenic bacteria in suppressing immunity through various mechanisms, it is largely unknown how T3SS effectors from symbiotic rhizobia contribute to mutualistic interactions.

T3SS effectors of the YopT–type family, such as YopT of *Yersinia pestis*, AvrPphB of *Pseudomonas syringae* pv. *phaseolicola* and rhizobial NopT proteins, are evolutionary related cysteine proteases (Shao et al., 2002; Dai et al., 2008). YopT cleaves Rho family GTPases leading to their inactivation to disrupt the actin cytoskeleton of human host cells (Shao et al., 2003a). AvrPphB can proteolytically cleave Arabidopsis receptor–like cytoplasmic kinase family proteins including PBS1, PBS1-like proteins and BIK1, to suppress PTI (Shao et al., 2003b; Zhang et al., 2010). Cleavage of PBS1 kinase by AvrPphB can be regarded as a "decoy strategy" as it is associated with RPS5 (RESISTANCE TO PSEUDOMONAS SYRINGAE5)-mediated ETI (Shao et al., 2003b). Depending on the host legume, the NopT effector protease of *Sinorhizobium fredii* NGR234 can have an opposite function in regulating symbiosis (Dai et al., 2008; Kambara et al., 2009). The heterologous expression of NopT from NGR234 in *S. fredii* USDA 257 severely blocks nodulation in soybean Nanfeng 15 but not in other soybean cultivars (Khan et al., 2022), implying that NopT can act as an Avr effector. In contrast, NopT positively regulates nodule formation in the interaction between *S. fredii* HH103 and soybean Suinong 14 (Li et al., 2023). NopT from *Bradyrhizobium* sp. ORS3257 promotes rhizobial infection in nodules of *Aeschynomene indica* (Teulet et al., 2019). NopT proteases have been biochemically characterized. Some exhibit autocleavage activity and are subsequently acylated at the newly formed N-terminus (Dai et al., 2008; Dowen et al., 2009; Kambara et al., 2009; Fotiadis et al., 2012; Khan et al., 2022). Recently, soybean PBS1-1 and two proteins in *Robinia pseudoacacia*

were identified as NopT targets (Luo et al., 2020; Khan et al. 2022; Li et al. 2023). However, at the molecular level, it remains largely unknown how NopT modulates rhizobial infection and whether NopTs from different rhizobial strains differ in their effector activities.

A challenge in the investigation of rhizobial effectors lies in the availability of suitable assays and plants with which effector activities can be characterized. In this study, we took advantage of the observation that ectopic expression of NFR1 and NFR5 in *N. benthamiana* leaves induces programmed cell death (Madsen et al., 2011). We hypothesized that this response could be modulated by co-expressed rhizobial effectors. Among the 15 known or putative T3SS effectors of *S. fredii* NGR234, only NopT could specifically suppress NFR1/NFR5-induced cell death. This observation suggested that NopT is an effector associated with NFRs. Subsequent experiments demonstrated that NopT interacts with both NFR1 and NFR5 at the plasma membrane and proteolytically cleaves NFR5 at the juxtamembrane (JM) domain to suppress NF-mediated host responses. NFR1 phosphorylates the full-length NopT, thereby inactivating its protease activity. However, the autocleaved NopT form of *S. fredii* NGR234 retains the ability to cleave NFR5 but loses its ability to interact with NFR1. Intriguingly, various *Sinorhizobium* strains possess only truncated versions of NopT (related to autocleaved NopT of NGR234) which can evade the inactivation by NFR1. We present in this study a model of mutual regulation, in which the rhizobial effector NopT directly targets NFR5 to dampen symbiotic signaling, whereas NFR1-mediated phosphorylation of NopT counteracts NFR5 cleavage. Our work provides essential insights into the intricate interplay between legumes and rhizobia and shows an example of how a rhizobal effector fine-tunes NF signaling by directly targeting NFRs, and how an NFR inactivates the enzymatic activity of the effector through phosphorylation.

Results

NopT expression in *N. benthamiana* suppresses the NFR1/NFR5-induced cell death response

To examine the role of effector proteins in regulating rhizobial infection, 15 effector genes (Kimbrel et al., 2013) were cloned from *S. fredii* NGR234, a strain with an exceptionally broad host-range. Initial experiments were performed to screen the effector proteins for their ability to suppress or enhance the NFR1/NFR5–triggered cell death response of *N. benthamiana* leaves. In this experiment, each effector was co-expressed with NFR1/NFR5 (Fig. S1A–S1C). Only NopT, a cysteine protease belonging to the YopT family (Shao et al., 2002; Dai et al., 2008), could suppress NFR1 and NFR5-induced cell death (Fig. 1A and S1D–S1F). Interestingly, NopT reduced protein abundance of the intact NFR5 when co–expressed with NFR1 (Fig. S1E), suggesting that NopT promotes proteolytic degradation of NFR5. Cys-93 of NopT is an amino acid residue known to be essential for the protease activity of this effector (Dai et al., 2008; Kambara et al., 2009). In contrast to the wild-type NopT protein, expression of the protease-dead $NopT^{C93S}$ form in *N. benthamiana* did not result in suppression of cell death induced by NFR1/NFR5 (Fig. 1B), indicating that the protease activity of NopT is essential for the observed cell death-suppressing activity of NopT. In contrast to NopT, NopM, an effector protein from *S. fredii* NGR234 reported to possess E3 ligase activity (Xin et al., 2012), induced cell death when expressed in *N. benthamiana* leaves under our test conditions (Fig. 1C).

We also tested whether the cell death-suppressing effect of NopT was specific for NFR1/NFR5 expression or whether NopT could act generally to suppress cell death. In addition to NopM, we examined various proteins known to induce cell death when expressed in *N. benthamiana* leaves, namely Avr3a and R3a (Bos et al., 2006), apoptosis regulator BAX (Bcl-2-associated X protein) (Gan et al., 2009), INF1, an

elicitor from *Phytophthora infestans* (Vleeshouwers et al., 2006) and Arabidopsis AtCERK1 (Cao et al., 2014) (Fig. 1C). In contrast to the NFR1/NFR5–induced cell death, expression of NopT was unable to suppress cell death when each of these proteins was expressed in *N. benthamiana* leaves (Fig. 1D). Hence, the effect of NopT appears to be specific for the NFRs. These results suggested that the effector protease NopT could act directly on NFR1 and/or NFR5.

NopT interacts with NFR1 and NFR5

Autocleaved NopT of *S. fredii* NGR234 contains acylation sites required for lipidation and subsequent plasma membrane localization (Dowen et al., 2009; Khan et al., 2022). To investigate whether NopT interacts with NFR1 and NFR5, we first used *in vivo* bimolecular fluorescence complementation (BiFC) analysis. NopT, NFR1 and NFR5 were C-terminally tagged with nYFP and cYFP. Fluorescence signals representing direct NopT-NFR1, NopT-NFR5 and NopT-NopT interactions were detected at the plasma membrane of *N. benthamiana* (Fig. 2A and 2B). Interactions between NopT and NFR1 and NFR5 were further verified using a Split-luciferase (Split–LUC) complementation assay (Fig. 2C). Co-expression of NopT-cLUC and NFR1-nLUC or NFR5-nLUC produced strong luminescence signals in transformed leaf discs compared with the negative control expressing AtFLS2-nLUC (Arabidopsis FLAGELLIN SENSING2) and NopT-cLUC (Fig. 2C).

It is known that acylation of NopT can alter its subcellular localization (Dowen et al., 2009; Khan et al., 2022). Here, we performed Split-LUC assays to examine the interaction between NFR1/NFR5 and $NopT^{G50A/C51A/C52A}$, a modified NopT form lacking acylation sites. Compared to the wild-type form ($NopT^{WT}$), the interactions between $NopT^{G50A/C51A/C52A}$ and NFR1/NFR5 were significantly reduced in Split-LUC assays (Fig. S2A and S2B). However, the protease-dead NopT form ($NopT^{C93S}$) showed interactions with NFR1 and NFR5 that were not different from $NopT^{WT}$ (Fig. S2C). These results were further confirmed by a co-immunoprecipitation (co-IP)

experiment with *N. benthamiana* leaves co-expressing FLAG-tagged NopT with C-terminally HA-tagged NFR1 or NFR5. Both NFR1 and LjNFR5 could be co-precipitated by an anti-FLAG antibody when the sample contained NopT-FLAG (Fig. 2D). Overall, the identified physical interactions between NopT and NFR1/NFR5 indicated that NopT targets NFRs and that NFR5 and/or NFR1 may be proteolytically cleaved by NopT.

NopT proteolytically cleaves NFR5 at the JM domain

A previous study has shown that NopT is autocleaved at its N-terminus to form a processed protein that lacks the first 49 amino acid residues (Dai et al., 2008). To test whether NopT could proteolyze NFR1 and/or NFR5, NopT was co-expressed with NFR1-GFP and NFR-GFP fusion proteins in *N. benthamiana* leaves. The expressed proteins were separated by SDS-PAGE and subjected to immunoblotting. Proteolytic cleavage of NFR5-GFP but not NFR1-GFP was observed in the presence of co-expressed NopT, whereas protease-dead $NopT^{C93S}$ showed no effect (Fig. 3A and S3A). A similar *in vivo* cleavage assay with transgenic *L. japonicus* roots also showed that expression of NopT but not $NopT^{C93S}$ caused proteolytic cleavage of NFR5 (Fig. 3B). Based on the molecular weight changes, the cleavage site in NFR5 was predicted to occur within the cytoplasmic domain (CD) of NFR5. To further explore NFR5 cleavage by NopT, the CD of NFR5 (Strep-$NFR5^{CD}$-HA) and NopT-FLAG or protease-dead $NopT^{C93S}$-FLAG were co-expressed in *Escherichia coli* cells. Immunoblotting results with an anti-HA antibody showed that the active NopT protease cleaved $NFR5^{CD}$ resulting in a ~5 kDa smaller protein. However, when the CD of NFR1 was co-expressed with NopT in the same experiment, no NFR1 cleavage was detected (Fig. 3C and 3D). Migration of the bands representing full-length NopT or $NopT^{C93S}$ was significantly retarded on the gel when the CD of NFR1 was co-expressed (Fig. 3C), suggesting that NopT was phosphorylated by NFR1 in *E. coli*.

The NFR5^{CD} cleavage product with a ~5 kDa lower molecular weight in the cleavage assay suggested that the cleavage site is located within the juxtamembrane (JM) domain of NFR5. To test this hypothesis, we replaced the JM with the SUMO tag to creat SUMO-NFR5^{KC}-HA (KC, kinase domain and C-terminal tail region, a modified NFR5^{CD} without the JM) for proteolytic assay. Indeed, immunoblot analysis showed that co-expressed NopT was unable to cleave SUMO-NFR5^{KC}-HA (Fig. S3B). The JM domain of NFR5 was then fused to SUMO and GFP to create a recombinant protein, SUMO-NFR5^{JM}-GFP. In an *in vitro* cleavage assay with recombinant proteins from *E. coli*, GFP was immunodetected in the flow though sample when SUMO-NFR5^{JM}-GFP was incubated with NopT but not with NopT^{C93S} (Fig. 3E). The interaction between NopT^{C93S} and SUMO-NFR5^{JM}-GFP was confirmed by an *in vitro* pull-down assay (Fig. S4). Overall, these data strongly indicate that the cleavage site of NFR5 for NopT is located in its JM domain.

The cleavage of NFR5 by NopT is dependent on multiple residues of the JM domain

The “DKLLSGV” motif in the JM domain of NFR5 (residues Asp-288 to Val-294; Fig. S5) shows highest similarity with the autocleavage region of NopT (DKMGCCA). However, a protein variant of NFR5^{CD} in which the “DKLLSGV” motif was replaced by 7 alanine residues could still be cleaved by NopT (Fig. S6A). Similar to NopT, the AvrPphB effector of *P. syringa* has an autocleavage site (Shao et al., 2003b). We therefore also examined a version of NFR5^{CD} in which the "DKLLSGV" motif was replaced by that of AvrPphB. In the cleavage assay with *E. coli* cells, AvrPphB did not cleave NFR5^{CD}. However, the modified NFR5^{CD} form with the 7 residues from AvrPphB was cleaved by AvrPphB and the cleavage product had a lower molecular weight than that formed by NopT (Fig. S6A). These findings indicated that the cleavage site for NopT is located upstream of the "DKLLSGV" motif in NFR5.

As mentioned above, NopT undergoes autocleavage but it is not clear whether this is due to intermolecular or intramolecular proteolysis. In addition to Cys-93, His-205 and Aps-220 of NopT are conserved catalytic residues (Dai et al., 2008; Kambara et al. 2009). Therefore, NopT forms lacking these catalytic residues were co-expressed with NopT in *E. coli*. The immunoblot analysis showed that NopT could not proteolyze NopT^{C93S}, NopT^{H205A} or NopT^{D220A} (Fig. S6B), suggesting that NopT autocleavage is due to intramolecular proteolysis. Hence, the residues at the autocleavage site of NopT may not help to predict the cleavage site of NopT substrates.

In an attempt to define the NopT cleavage site in NFR5, we created a series of modified NFR5 forms covering the JM domain of NFR5 (Val-269 to Cys-320) and the first seven amino acid residues of the kinase domain (Lys-321 to Tyr-327). Initially, 17 variants of NFR5^{CD} were created in which three adjacent amino acids in the JM domain were replaced with three alanine residues. When these proteins were co-expressed with NopT in *E. coli*, all 17 NFR5^{CD} variants could be cleaved by NopT but not NopT^{C93S} (Fig.S6C-S6F). In a similar experiment, we created seven NFR5^{CD} forms which contained a deletion in the JM domain of 10 residues each. Surprisingly, cleavage products were still observed for all seven examined proteins (Fig. S6G). These results suggest that the JM domain may have multiple sites that can be cleaved by NopT, which is different from the specific cleavage site identified for AvrPphB. In another experiment, recombinant His-SUMO-NFR5^{CD}-GST protein was co-expressed with NopT in *E. coli* and its cleavage product was subjected to N-terminal protein sequencing using Liquid Chromatography Mass Sprectrometry (LC-MS) analysis. Based on alignment of identified peptides, the NopT cleavage site in NFR5 was mapped to four basic amino acids in the JM domain (RRKK; amino acid residues 271-275) (Fig. S7). However, this result was not consistent with the observation that NopT expressed in *E. coli* could still proteolyze a co-expressed NFR5^{CD} form in which the residues from Tyr-268 to Leu-277 were deleted (Fig. S6G). Overall, the experiments performed suggest that NopT preferentially proteolyzes NFR5 at the

RRKK motif, but other sites in the JM domain can also be cleaved by NopT. Since NFR5 belongs to a subfamily of LYK family proteins that lacks kinase activity (Yang et al., 2022), we wondered whether NopT could proteolyze other LYK proteins of this subfamily, which might be helpful to characterize the biochemical function of NopT. We therefore investigated whether the CDs from Arabidopsis AtLYK5, *L. japonicus* LjLYS11 and *M. truncatula* MtNFP expressed in *E. coli* can be proteolyzed by NopT. As shown in Fig. S8, NopT, but not NopT^{C93S}, was able to cleave the CDs of AtLYK5 and LjLYS11. Replacement of the JM domain in NFR5^{CD} with the JM domain from either AtLYK5 or LjLYS11 resulted in cleavage by NopT (Fig. S8). These data show that NopT cleaves AtLYK5 and LjLYS11 at their JM domains. Based on sequence analysis of the JM region of NFR5 and its homologous proteins, five conserved residues (Ser-283, Gly-294, Tyr-304, Ala-310, Thr-311) were identified and mutated as NFR5$^{CD\text{-}5m}$ for the proteolytic assay (Fig. S5B). As shown in Fig. 3F, NFR5$^{CD\text{-}5m}$, a NFR5^{CD} variant with point mutations of S283Y, G294Q, Y304S, A310I, and T311Y, could not be cleaved by NopT. Interestingly, NopT could not proteolyze MtNFP^{CD} (Fig. 3G). We then swapped the JM domains in NFR5^{CD} and MtNFP^{CD}, generating NFP^{JM}-NFR5^{KC} and NFR5^{JM}-NFP^{KC} (KC stands for the kinase domain and the C-terminal tail region). As shown in Fig. 3G, NopT could proteolyze NFP^{JM}-NFR5^{KC} but not NFR5^{JM}-NFP^{KC} in *E. coli*. In an *in vitro* cleavage assay, the cleavage product of SUMO-NFP^{JM}-GFP proteolyzed by NopT was detected in the flow though sample (Fig. S9). These data suggest that the cleavage of NFR5 by NopT depends on the conformational structure of NFR5^{KC} and/or other specific amino acids in NFR5^{KC}. We then investigated whether two additional recombinant proteins with large swapping regions in NFR5^{CD} and NFP^{CD} (NFR5$^{268\text{-}445}$-NFP$^{458\text{-}595}$ and NFP$^{270\text{-}457}$-NFR5$^{456\text{-}595}$) could be cleaved in the *E. coli* proteolysis test (Fig. S10). Notably, both proteins were cleaved by NopT, suggesting that a specific conformation of the NopT substrate is required for proteolysis. Taken together, we concluded from our experiments that NopT can proteolyze NFR5 at the JM domain and that mutiple nonadjacent residues in NFR5^{JM} in combination with a specific KC conformation are required for proteolysis.

NopT phosphorylated by NFR1 is proteolytically inactive

The perception of rhizobial NFs by the heterocomplex of NFR1 and NFR5 involves trans-phosphorylation events from the NFR1 kinase to the pseudo-kinase NFR5 (Madsen et al., 2011). Since NopT is associated with both NFR1 and NFR5, we hypothesized that NopT is a phosphorylation target of NFR1, which may interfere with transphosphorylation events between the two receptors. $NopT^{C93S}$ was therefore expressed in *L. japonicus* wild-type and *NFR1* knockout mutant plants (*nfr1-1*) and analyzed on Zn^{2+}-Phos-tag gels. On such gels, a Zn^{2+}-Phos-tag bound phosphorylated protein migrates slower than its unbound nonphosphorylated form. Slower migrating bands corresponding to phosphorylated $NopT^{C93S}$ were observed, particularly when wild-type plants were inoculated with rhizobia (Fig. 4A and 4B). These findings indicated that NopT phosphorylation *in planta* is largely dependent on NFR1 and that the protein was probably phosphorylated at multiple sites.

Next, we performed assays to investigate whether expressed $NFR1^{CD}$ directly phosphorylates co-expressed NopT. $NFR5^{CD}$ and a kinase-inactive $NFR1^{CD}$ form ($NFR1^{CD\text{-}K351E}$; Lys-351 is a conserved residue required for ATP binding) were included into these experiments. When $NFR1^{CD}$ was expressed in *E. coli*, extracted NopT (Fig. 3C and 4C) and $NFR5^{CD}$ (Fig. S11) exhibited retarded migration on SDS-PAGE gels, indicating that NFR1 was able to phosphorylate both proteins. A band shift was observed when the phosphorylated full-length NopT was *in vitro* dephosphorylated by calf intestinal alkaline phosphatase (CIAP). However, the CIAP treatment caused no obvious band shift of the autocleaved NopT form (Fig. 4C). The phosphorylation sites of NopT were then identified using an *in vitro* phosphorylation assay followed by LC-MS analysis. Several serine and threonine residues in NopT were identified to be phosphorylated by $NFR1^{CD}$ (Table S1). Taken together, these results showed that full-length NopT is a phosphorylation target of the NFR1 kinase.

Finally, we wondered whether NopT phosphorylation by NFR1 influences its proteolytic activity. Plasmids encoding NopT variants were constructed in which the phosphorylated residues were substituted to either alanine (to block phosphorylation) or aspartate (to mimic the phosphorylation status). The different NopT forms were then expressed in *E. coli* to analyze NopT autocleavage and proteolysis of co-expressed $NFR5^{CD}$. Aspartate substitutions at three phosphorylation sites of NopT (Thr-97, Ser-119 and Thr-257) resulted in the loss of the autoproteolytic activity, as well as the ability to cleave+ $NFR5^{CD}$ (Fig. 4D). In contrast, corresponding NopT proteins with alanine substitutions retained autocleavage activity and the ability to proteolyze $NFR5^{CD}$ (Fig. 4D). These data indicate that phosphorylation of full-length NopT by NFR1 inhibits its proteolytic activity, thereby keeping NopT unprocessed and NFR5 uncleaved.

NopT dampens rhizobial infection

As NopT of *S. fredii* NGR234 could directly target and cleave NFR5, we expected that NopT may be an important player regulating rhizobial infection in legumes. NF signaling is known to function during early stages of rhizobial infection (Geurts et al., 2005; Wang et al., 2012; Cai et al., 2018). We focused our experiments on early stages of rhizobial infection. Inoculation of *L. japonicus* plants with a GFP- or GUS-labelled *nopT* mutant of NGR234 (NGR234 Δ*nopT*) resulted in a massive infection of root hairs, whereas infection by the NGR234 wild-type strain was less frequent (Fig. 5A and 5C). We also performed experiments with *L. japonicus* plants containing *pNIN*:*GUS* which exhibit β-glucuronidase (GUS) activity when the *NIN* (NODULE INCEPTION) promoter activity is induced by NF signaling (Schauser et al., 1999). GUS staining of roots showed that the *NIN* promoter activity was stronger in response to NGR234Δ*nopT* inoculation relative to inoculatioin by wild-type NGR234 (Fig. 5B and 5D). Likewise, inoculation with NGR234Δ*nopT* resulted in an increased number of nodule primordia (Fig. 5G). In contrast, over-expression of NopT under the control of the T7 promoter in the NGR234 parent strain reduced the number

of nodule primordia when compared to inoculation with the wild-type strain (Fig. 5G). These findings indicate that NopT negatively influences symbiosis at early symbiotic stages. However, we could not find any uninfected (empty) nodules when roots were inoculated with these strains.

To confirm that the massive infection of roots by NGR234Δ*nopT* is due to the loss of NopT, we complemented the NGR234Δ*nopT* by expressing wild-type NopT. The *L. japonicus* plants inoculated with this complemented strain had fewer infection foci, indicating restoration of the wild-type phenotype (Fig. 5E). We also tested whether the proteolytic activity of NopT affected rhizobial infection. The protease-dead version of $NopT^{C93S}$ and three NopT forms with phospho-mimimetic residues (i.e., $NopT^{T97D}$, $NopT^{S119D}$, and $NopT^{T257D}$ lacking proteolytic activity) were individually expressed in NGR234Δ*nopT*. Compared with the high number of infection foci induced by NGR234Δ*nopT* in *L. japonicus* plants, inoculation with these strains resulted in significantly fewer infection foci, but more than with the wild-type strain (Fig. 5E).

We also expressed *nopT* under the control of a ubiquitin promoter in hairy roots of *L. japonicus* and inoculated the transgenic roots with DsRed-labeled *M. loti* MAFF303099, which does not possess a *nopT* gene in its genome. As shown in Fig. 5F, reduced numbers of infection foci and infection threads were observed in the NopT expressing roots, indicating that NopT negatively affects the symbiosis between *L. japonicus* and *M. loti* strain.

To investigate whether the cleavage of NFR5 by NopT reduces rhizobial infection of *L. japonicus* roots, *NFR5* and $NFR5^{5m}$ (uncleavable variant with 5 amino acid substitutions in the JM domain; Fig. 3F) under the control of the native *NFR5* promoter, were expressed in hairy roots of *NFR5* knockout mutant plants (*nfr5-3*). NFR5 expression resulted in numerous infections and a significant increase of infection foci was observed upon inoculation with the NGR234Δ*nopT* mutant (Fig.

5H). However, $NFR5^{5m}$ expression showed no effects on rhizobial infection (Fig. S12), suggesting that the amino acid substitutions in $NFR5^{5m}$ caused a conformational change that rendered the protein inactive in symbiotic signaling. As the $NFR5^{JM}$-NFP^{KC} fusion protein was not cleaved by NopT (Fig. 3G), we also constructed hairy roots of *nfr5-3* mutant plants in which *NFR5-NFP*^{KC} (NFR5 variant with its KC domain replaced by the KC of MtNFP) was expressed under the control of the *NFR5* promoter. Remarkably, inoculation of these plants showed no difference between NGR234Δ*nopT* and the NGR234 wild-type strain in terms of rhizobial infection foci (Fig. 5H), suggesting that the cleavage of NFR5 by NopT reduced the degree of rhizobial infection. Taken together, these data indicate that the protease activity of NopT, its phosphorylation status and the proteolysis of the NFR5 target are important for the regulation of rhizobial infection.

NopT from other *S. fredii* strains also cleave NFR5

Since NopT of *S. fredii* NGR234 ($NopT_{NGR234}$) cleaves NFR5, we wondered whether homologs from other rhizobial species also possess such a proteolytic activity. Phylogenetic analysis showed that NopT proteins of *Sinorhizobium* and *Bradyrhizobium* are located in different clades (Fig. S13). *B. diazoefficiens* USDA110, a typical *Bradyrhizobium* strain used to study nodulation of soybeans, produces two NopT proteins (Fotiadis et al., 2012). In contrast to $NopT_{NGR234}$, however, neither $NopT1_{USDA110}$ nor $NopT2_{USDA110}$ were able to cleave co-expressed NFR5 in *E. coli* (Fig. 6A). This finding suggests that NopT homologs from *Bradyrhizbium* species have lost the ability to cleave NFR5 and probably act on other, unknown host target proteins. The genome of various *Sinorhizobium* species (e.g., *S. fredii* USDA257 and S. *fredii* HH103) possess genes that encode truncated NopT forms, which are almost identical to the autocleaved version of $NopT_{NGR234}$ (Khan et al., 2022). Remarkably, $NopT_{USDA257}$ and $NopT_{HH103}$ were both able to cleave NFR5 *in E. coli* (Fig. 6A). However, both NopT proteins were unable to suppress cell death triggered by NFR1 and NFR5 expression in *N. benthamiana* leaves (Fig. 6B).

Moreover, expression of $NopT_{USDA257}$ in NGR234Δ*nopT* had no effect on the infection ability of NGR234Δ*nopT*, as observed in inoculation tests with the *L. japonicus* line containing *pNIN*:*GUS* (Fig. 6C and 6D). These results suggest that $NopT_{USDA257}$ and $NopT_{HH103}$ exhibit similar proteolytic activity to $NopT_{NGR234}$, but target different host proteins to regulate rhizobial infection.

Discussion

Plant-microbe interactions are complex, employing distinct "chemical weapons" or strategies to communicate mutually, thereby securing more resources for their survival (Jones and Dangl, 2006; Schubert et al., 2020). T3SS effectors of phytopathogenic bacteria are injected into plant cells to facilitate bacterial infection by targeting host proteins of the plant's immune system, thereby suppressing PTI (Jones and Dangl, 2006; Tang et al., 2017). However, the role of rhizobial T3SS effectors in regulating the mutualistic symbiosis between legumes and rhizobia remains largely unknown. The aim of this study was to gain essential insights into the regulation mechanisms by which rhizobial effectors act directly on symbiotic signaling pathways to promote or dampen infection of host cells.

Understanding how plants recognize different microbes as "friends" or "foes" is a central question in biology. The perception of microbial signals by plant receptor proteins is essential for triggering specific signaling pathways to resist invading pathogens or to establish symbiosis with beneficial microbes (Zipfel and Oldroyd, 2017). Direct targeting of these receptors by T3SS effectors represents an efficient strategy of phytopathogenic bacteria to suppress PTI and promote bacterial infection. In the well-studied *Arabidopsis-Pseudomonas syringae* interaction, T3SS effectors target flagellin receptor FLS2 and its coreceptor BAK1 (BRI1-[Brassinosteroid insensitive1]-associated receptor kinase 1) to suppress flagellin-induced PTI (Zipfel et al., 2004; Sun et al.,

2013). For example, AvrPto targets FLS2 and HopB1 cleaves BAK1 (Xiang et al., 2008; Li et al., 2016). Likewise, AvrPtoB, an E3 ligase in *P. syringae*, targets FLS2 to promote its degradation and suppress PTI (Goehre et al., 2008). Despite the evolutionary importance of T3SS effectors in targeting host receptors, we were surprised to find that NopT, a rhizobial member of the C58 protease effector family, can directly target NFRs and manipulate the symbiotic signaling pathway in legumes. The interaction between NopT of *S. fredii* NGR234 and NFRs of *L. japonicus* was identified by using a unique screening system, in which co-expression of NFR1/NFR5 in *N. benthamiana* leaves leads to cell death. NopT, but not other effectors of NGR234, could suppress this cell death response. Consistent with these initial observations, inoculation of *L. japonicus* with the *S. fredii* NGR234Δ*nopT* mutant resulted in increased infection of *L. japonicus* roots. Moreover, over-expression of NopT in the roots was found to reduce rhizobial infection by *M. loti*. The interaction between NopT and NFR1/NFR5 was verified by BiFC, Split-LUC and co-IP experiments.

Interestingly, using different assays, we found that NopT cleaves NFR5 at the JM domain. However, the efficiencies of NopT cleavage of NFR5 in *L. japonicus* and *N. benthamiana* were different (Fig. S14), which could be related to the uncontrollable activation of NFRs in *N. benthamiana* or phosphorylation of NopT by another kinase leading to decreased proteolytic activity. The modification of five conserved residues in the JM domain and the replacement of $NFR5^{KC}$ by NFP^{KC} resulted in $NFR5^{CD}$ forms that were resistant to proteolysis by NopT in *E. coli* cells. These results suggest that cleavage of NFR5 depends on both the JM domain and the KC region. Although belonging to the same protease family, the NopT cleavage site in NFR5 was found to be polybasic as in YopT substrate (Shao et al., 2003a; Schmidt, 2011), whereas the cleavage site of AvrPphB substrate is canonical with seven adjacent amino acids involved (Kim et al., 2016). These differences

reflect a broad variety of YopT-type effector proteases and their substrates in host cells. Our study shows, that NopT targets the NFR1/NFR5 complex thus reduces NF signaling and formation of nodule primordia in *L. japonicus*. NopT-NFR interactions may reflect a regulation mechanism to prevent rhizobial hyperinfection in host species other than *L. japonicus*.

Similar to the *Pseudomonas* effector AvrPphB, NopT of *S. fredii* NGR234 is able to cleave soybean PBS1-1 and expression of this effector in *S. fredii* USDA257 negatively influences symbiosis with certain soybean cultivars (Khan et al., 2022). Indeed, NopT of NGR234 acts as an Avr effector in some nonhost plants. Transient expression of NopT of strain NGR234 in Arabidopsis and tobacco triggers strong immune responses and cell death (Dai et al., 2008; Kimbrel et al., 2013; Khan et al., 2022; Fig. S15). In Arabidopsis, NopT-induced cell death was found to be dependent on the PBS1-1 kinase and the resistance protein RPS5 (Khan et al., 2022). Likewise, when constitutively expressing NopT and NopT^{C93S} in *L. japonicus*, we only obtained stable transgenic lines expressing NopT^{C93S}, indicating that the protease activity of NopT had a negative effect on plant development. In contrast, generation of hairy roots expressing NopT was possible. Such differences may be explained by different NopT substrates in roots and aerial parts of the plant. Indeed, our study shows that NopT not only cleaves NFR5 but is also able to proteolyze Arabidopsis AtLYK5 and *L. japonicus* LjLYS11. These two receptors possess chitin-binding affinities and trigger PTI responses (Cao et al., 2014; Gysel et al., 2021). NFR5, AtLYK5, and LjLYS11 are kinase-dead LYKs belonging to the same LYK subfamily. Thus, NopT appears not only to suppress NF signaling, but may also interfere with signal transduction pathways related to plant immunity. Depending on the host legume species, NopT could suppress PTI or induce ETI, thereby modulating rhizobial infection and nodule formation. Interactions between NopT and proteins related to the plant immune system may represent an important evolutionary driving force for

host-specific nodulation and explain why the presence of NopT in NGR234 has a negative effect on symbiosis with *L. japonicus* but a positive one with other legumes.

The regulation of kinase-dead pseudokinases in plants may be more complex compared to the well-studied control of protein kinase activities by phosphorylation. The cleavage of kinase-dead receptors may be an overlooked strategy to regulate their function in plant biology. Regulation of protein activities by cleavage is well studied in animals, e.g., for Notch signaling, where proteolysis of Notch molecules leads to downstream signaling (Kopan and Ilagan, 2009). Arabidopsis BAK1 undergoes proteolytic cleavage, which is important for both brassinosteroid signaling and induction of PTI responses (Zhou et al., 2019). The cytoplasmic domain of NFR5 is a pseudokinase that contributes to activation of NF signaling. Our work indicates that NopT proteolytically cleaves NFR5 and suppresses NF signaling. Such a fine-tuning process could be advantageous for the symbiosis in host plants other than *L. japonicus*, for example to prevent hyperinfection. However, the precise function of NFR5 cleavage by NopT and the fate of the released cytoplasmic domain remain to be clarified.

Mutual regulation between T3SS effectors and host target proteins has been investigated for various plant-pathogen interactions. For example, the conserved *Pseudomonas* effector AvrPtoB can directly ubiquitinate the key components of plant immunity to promote bacterial virulence (Goehre et al., 2008). However, the activity of AvrPtoB in promoting virulence could either be enhanced or dampened by host proteins. AvrPtoB can be phosphorylated by SnRK2.8 to promote its virulence activity (Lei et al., 2020). On the other hand, the plant lectin receptor-like kinase LexRK-IX.2 and the Pto kinase phosphorylate AvrPtoB to inactivate its ubiquitin E3 ligase activity and undermine the effector's ability to suppress PTI (Ntoukakis et al., 2009; Xu et

al., 2020). A similar strategy is used by NFR1 to inhibit the protease activity of NopT *via* phosphorylation. NFR1 expressed in *E. coli* phosphorylates full-length NopT of *S. fredii* NGR234 at several residues. Three NopT forms with a phosphomimetic substitution (i.e., $NopT^{T97D}$, $NopT^{S119D}$, and $NopT^{T257D}$) lacked autoproteolytic activity and the ability to cleave NFR5. The expression of these NopT variants in the NGR234Δ*nopT* mutant showed little effects in comparison with expression of wild-type NopT. These data suggest that *L. japonicus* utilizes NFR1 to phosphorylate NopT in order to dampen its catalytic activity and protect NFR5 from cleavage, which favors rhizobial infections. However, $NopT^{\Delta N50}$, which is similar to autocleaved NopT, retained the ability to interact with NFR5 but not with NFR1. Moreover, full-length NopT, but not autocleaved NopT, migrated slower on gels when $NFR1^{CD}$ was co-expressed in *E. coli*, suggesting that autocleaved NopT may escape being phosphorylated and inactivated by NFR1. Future studies are required to explore the interactions between acylated NopT and NFR1. When expressed in *N. benthamiana*, GFP-tagged NopT forms lacking their autocleavage site (and thus non-acylated) were found to be localized within the cytoplasm, whereas NopT was targeted to the plasma membrane (Khan et al., 2022). Accordingly, NopT without acylation sites showed weaker interactions with NFRs in our study, suggesting that acylation of NopT, leading to plasma membrane location, promotes NopT-NFR interactions.

NopT homologs vary in different *S. fredii* strains. USDA257 and HH103 produce truncated NopT versions different from NGR234 due to a 19-bp deletion (Khan et al., 2022). Accordingly, NopT of these strains lacks autocleavage and acylation sites and possess a different N-terminal secretion signal sequence (Akeda and Galán, 2005). Nevertheless, $NopT_{HH103}$ is a functional T3SS effector as mutant analysis indicated a symbiosis-promoting role in certain soybean cultivars (Li et al., 2023). Similar to $NopT_{NGR234}$, $NopT_{USDA257}$ and $NopT_{HH103}$ were able to cleave NFR5 in *E. coli*. Since

$NopT_{USDA257}$ and $NopT_{HH103}$ cannot be acylated, they likely accumulate in the cytoplasm of host legumes and are therefore less efficient in cleaving plasma membrane-bound NFR5 in comparison to acylated $NopT_{NGR234}$. This could also explain why $NopT_{USDA257}$ was unable to suppress cell death triggered by NFR1/NFR5 in *N. benthamiana* leaves. It can be expected that NFR1 does not interact with and phosphorylate $NopT_{USDA257}$ or $NopT_{HH103}$, as these effectors are similar to $NopT^{\Delta N50}$ of NGR234, which cannot interact with NFR1. Consistent with these findings, expression of $NopT_{USDA257}$ in NGR234*ΔnopT* did not alter the infection phenotype of NGR234*ΔnopT*. It can be hypothesized that the host targets of these truncated NopT effectors might be different from those of $NopT_{NGR234}$. *Bradyrhizobium* NopT effectors are also different from $NopT_{NGR234}$, as NopT of *B. diazoefficiens* USDA110 was unable to cleave NFR5). NopT effectors may play a crucial role in *Bradyrhizobium*-legume interactions. A *Bradyrhizobium* sp. ORS3257 mutant deficient in NopT production induced only ineffective nodules on roots of *Aeschynomene indica* and most of the formed nodules were not infected (Teulet et al., 2019). Overall, these findings indicate versatile functions of NopT homologs in different strains and suggest that NopT controls different regulation processes in specific host cells.

We present here a model of mutual regulation, in which NopT proteolyzes NFR5 to suppress NF signaling, whereas protease activity of full-length NopT is suppressed by NFR1 *via* phosphorylation (Fig. 6E). NopT impairs the function of the NFR1/NFR5 receptor complex. Cleavage of NFR5 by NopT reduces its protein levels. Possible inhibitory effects of NFR5 cleavage products on NF signaling are unknown but cannot be excluded. Inactivation of NopT protease activity *via* phosphorylation by kinases such as NFR1 appears to be a countermeasure of the host to enable symbiotic signaling and rhizobial infection. Such feedback regulation could be the result of evolutionary pressure to produce ‘improved’ NFRs, which are resistant to cleavage by NopT

and have an increased capacity to phosphorylate NopT. On the other hand, suppression of NopT protease activity by NFRs may drive broad-host-range strains such as NGR234 to produce higher levels and structurally modified NFs.

Taken together, this study provides insights into a legume-rhizobium interaction, in which the bacterium deploys an effector protease to dampen symbiotic signaling, while the host plant counteracts by phosphorylating the effector, leading to its inactivation. Our findings highlight the function of a bacterial effector protease in regulating a symbiotic signaling pathway in legumes. This opens up the perspective of developing specific kinase-interacting proteases to reprogram and fine-tune cellular signaling processes in general.

Materials and Methods

Germination and growth of *Lotus japonicus*

Lotus japonicus (ecotype Gifu B-129) was provided by the Center for Carbohydrate Recognition and Signaling (https://lotus.au.dk/), and used as wild-type for nodulation assays. The Gifu *pNIN*:*GUS* transgenic line and *nfr* mutants (*nfr1-1* and *nfr5-3*) were kindly provided by Dr. Jens Stougaard from the Aarhus University, Denmark (Madsen et al., 2003; Radutoiu et al. 2003; Heckmann et al., 2011). All *L. japonicus* seeds were treated with concentrated sulfuric acid for 10 min, followed by surface sterilization in 1% (w/v) NaClO for 8 min. After incubation at 4°C in the dark for 2 d, the seeds were placed on 0.8% (w/v) agar containing half-strength Murashige & Skoog (MS) medium for germination at 22°C for 2 d in the dark. Seedlings were then transferred to growth pots containing vermiculite supplied with half-strength B&D (Broughton & Dilworth) medium without nitrogen under long-day conditions (16-h

light/8-h dark) at 22°C. Ten-day-old seedlings were inoculated with rhizobial cultures (OD_{600}=0.02) for infection experiments.

Plasmid construction

All plasmids used in this study were generated using MultiF Seamless Assembly Mix (Abclonal, # RK21020). The plasmid pGWB514 was used as an original plasmid for construction of all binary vectors (Nakagawa et al., 2007). Briefly, different tags including HA tag, Myc tag, FLAG tag, Strep tag, nLUC, cLUC and GFP, were amplified using a forward primer containing a *Kpn*I site and ligated into pGWB514 digested with *Xba*I and *Sac*I using the seamless cloning method described above. The generated plasmids were named pG5XX-HA, pG5XX-Myc, pG5XX-FLAG, pG5XX-nLUC, pG5XX-cLUC, pG5XX-GFP, respectively. The coding sequences of *L. japonicus NFR1* and *NFR5* were cloned into pGWB514 and pG517 between *Xba*I/*Kpn*I to generate NFR1-HA and NFR5-Myc fusion constructs under the control of the cauliflower mosaic virus 35S promoter. The DNA fragment containing *pro35S*:NFR5-Myc-NosT was then amplified and cloned into pG514-NFR1 at *Sbf*I. The final plasmids contained *pro35S*:NFR1-HA-NosT and *pro35S*:NFR5-Myc-NosT. Rhizobial genes encoding effectors from *S. fredii* NGR234 were cloned into pG5XX-FLAG between *Xba*I/*Kpn*I. To detect the interaction between NFR1/NFR5 and NopT in *N. benthamiana*, the full-length *NFR1/NFR5*, *NopT* and *AtFLS2* coding sequences were cloned into pG5XX-Nluc, pG5XX-Nluc, pSPYCE(MR) and pSPYNE(R)173 (Waadt et al., 2008). For cleavage assays in *N. benthamiana* leaves, the *NFR5* and *NopT* coding sequences were cloned into pG5XX-FLAG GFP and pG5XX-Strep, respectively. For cleavage assays in *E. coli*, the sequence encoding the cytoplasmic domain of NFR5 was cloned into pACYC duet Strep-HA (Han et al., 2017), and the sequences encoding the kinase domain of NFR5 fused to the HA tag and the JM domain of NFR5 fused to the GFP tag were cloned into pSUMO. The point mutations in $NFR5^{CD}$ and *NopT* were created by site-directed mutagenesis PCR using the templates pACYC duet Strep-$NFR5^{CD}$-HA and pET28a NopT-FLAG . For NFR/NopT cleavage experiments with *L. japonicus* plants, NopT-FLAG or

680 NopT^{C93S}-FLAG was cloned into pUB-GFP between *Xba*I and *Kpn*I, and
681 35S-NFR5-Myc-NosT was cloned into pUB-NopT-GFP at *Pst*I. For NopT
682 phosphorylation experiments with *E. coli*, the sequence encoding the cytoplasmic
683 domain of NFR1 fused to a Myc tag was cloned into pCDF duet. For
684 complementation experiments with the NGR234Δ*nopT* mutant (Dai et al., 2008), a
685 1317-bp DNA fragment upstream of *NopT* and the coding sequence of a given *NopT*
686 sequence was fused using overlap PCR and cloned into pHC60 between *Xho*I and
687 *Kpn*I. For complementation experiments with the *nfr5-3* mutant, a 1316-bp *NFR5*
688 promoter DNA fragment was fused to NFR5-NFP^{KC} or NFR5^{5m}using overlap PCR
689 and cloned into pUB-Cherry between *Pst*I and *Kpn*I.

690 Transient gene expression in *Nicotiana* leaves

691 The plasmids of *INF1*, *Avr3*, *BAX*, and *R3a* for transient expression in *Nicotiana*
692 *benthamiana* were kindly gifted by Dr. Juan Du from Huazhong Agricultural
693 University. *Agrobacterium tumefaciens* strain EHA105 carrying various constructs
694 were mixed with an *Agrobacterium* culture harboring the P19 suppressor in an
695 infiltration buffer (10 mM $MgCl_2$, 10 mM MES-KOH pH 5.8 and 200 μM
696 acetosyringone). After incubation for 2 h at room temperature, *Agrobacterium*
697 cultures were infiltrated into the leaves of 4-week-old *N. benthamiana* and *N. tabacum*
698 plants. Leaves were harvested and analyzed two-days post inoculation. The cell death
699 suppression experiments with *N. benthamiana* plants were performed as described
700 previously (Wang et al., 2011).

701 Hairy root transformation

702 Hairy root transformation of *L. japonicus* plants was performed as described
703 previously (Li et al., 2018). In brief, surface-sterilized seeds were germinated and
704 grown on MS plates without sucrose (23°C in the dark for the first 3 days and 23°C at
705 a 16-h light/8-h dark period for the following 2 days). The seeds were then cut at the
706 middle of the hypocotyl and co-cultivated with *A. rhizogenes* LBA1334 carrying
707 pUB-GFP , pUB-NopT-FLAG-GFP, pNFR5:NFR5-mCherry,

pNFR5:NFR5^{5m}-mCherry and pNFR5:NFR5-NFP^{KC}-mCherry, respectively (23°C in the dark for the first 3 days and 23°C at a 16-h light/8-h dark period for the following 2 days). The plants were then transferred onto solid B5 medium. After about 15 days, non-fluorescent hairy roots (lacking expression of GFP or mCherry) were removed. Where indicated, the plants were inoculated with rhizobia: *S. fredii* NGR234, NGR234Δ*nopT* or *Mesorhizobium loti* MAFF303099, and analyzed at indicated time points.

Analysis of NFR5 cleavage by NopT and variants

In experiments with *E. coli*, Strep-NFR5^{CD}-HA or Strep-NFR5^{CD}-HA variants were co-expressed with NopT-FLAG or FLAG tagged NopT variant or AvrPphB-FLAG by using Duet vectors (Novagen; Han et al., 2017). Bacterial cultures were treated with 0.5 mM IPTG at 22°C for 15 h. After washing the bacterial cells with PBS buffer, the bacterial pellet was resuspended in extraction buffer consisting of Tris-HCl (pH 7.3), 150 mM NaCl, 5 mM EDTA, 0.5% (w/v) SDS and 0.5% (v/v) Triton X-100. After adding SDS loading buffer and boiling at 100°C for 5 min, the extracted proteins were subjected to immunoblot analysis using anti-HA-peroxidase (Sigma, clone 3F10) or anti-FLAG (Sigma, F1804) antibodies. An anti-groEL antibody (ABclonal, A0969) was used to confirm equal loading of proteins on gels.

For *in vitro* cleavage assays, His-SUMO-NFR5^{JM}-GFP and NopT-FLAG-His proteins were expressed in *E. coli* and purified. The reaction mixture contained 3 μg NopT-FLAG (or NopT^{C93S}-FLAG) and 1 μg SUMO-NFR5^{JM}-GFP in extraction buffer without SDS and EDTA. After incubation at 22°C for 7 h, 10 μL of a Ni-charged resin (GenScript, Cat. No. L00223) were added, and the cleavage products in the flow through were detected by immunoblot analysis using an anti-GFP antibody (ABclonal, AB_2770402).

To analyze cleavage of NFR5 in *L. japonicus* roots, hairy roots co-expressing NopT-FLAG or NopT^{C93S}-FLAG with NFR5-Myc were harvested at about 15 days after induction of hairy roots without rhizobia inoculation and subjected to

immunoblot analysis. Expressed proteins were extract by extraction buffer and immunodetected with anti-FLAG antibodies and anti-Myc (Bio-Legend, # 626808) antibodies.

For NFR5/NopT cleavage experiments with *N. benthamiana* plants, leaves expressing proteins (NopT-FLAG or NopT^{C93S}-FLAG with NFR5-GFP) were analyzed. Leaf discs were collected at 2 days post infiltration with agrobacteria and extracted in the extraction buffer (Tris-HCl (pH 7.3), 150 mM NaCl, 5 mM EDTA, 0.5% (w/v) SDS and 0.5% (v/v) Triton X-100) and 2% protease inhibitors (Sigma, P9599). NFR5 was immunodetected with anti-Myc and anti-GFP (ABclonal, AB_2770402) antibodies. The NopT or NopT^{C93S} were detected with anti-FLAG antibody . The actin proteins were detected with anti-Actin antibody (Abclonal, # AC009).

Phosphorylation assays

For NopT phosphorylation in *E. coli*, His-NFR1^{CD}-Myc or His-NFR1$^{CD-K351E}$-Myc was co-expressed with NopT-FLAG-His by using Duet vectors (Novagen). Protein expression was induced by 0.5 mM IPTG and cells were grown at 28°C for 18 h. After simultaneous purification of NFR1^{CD} and NopT using Ni-charged resin, the proteins were incubated with CIAP (TaKaRa, 2250B) at 37°C for 3 h. The mobility shifts of NFR1^{CD} and NopT were detected with anti-Myc (Bio-Legend, 626808) and anti-FLAG (Sigma, F1804) antibodies by immunoblot analysis.

In phosphorylation experiments with *L. japonicus* plants, NopT^{C93S}-FLAG was expressed in hairy roots of the *nfr1-1* mutant and wild-type plants, respectively. After removal of roots without fluorescence signals, plants were kept on half-strength B&D medium for 5 days. Roots were inoculated with *Mesorhizobium loti* MAFF303099 or treated with water. Total proteins were extracted using the extraction buffer (Tris-HCl (pH 7.3), 150 mM NaCl, 5 mM EDTA, 0.5% (w/v) SDS and 0.5% (v/v) Triton X-100) supplemented with 2% protease inhibitor cocktail (Sigma, P9599) and

2% phosphatase inhibitor cocktail (Yeasen, 20109-A). Proteins were then precipitated with TCA to remove various contaminants (e.g., EDTA and surfactant)s. Phosphorylation of the NopT^{C93S} protein was analyzed by 50 μM Zn^{2+}-Phos-tag SDS-PAGE gel (Kato & Sakamoto, 2019) and detected with the anti-FLAG antibody by immunoblot analysis. As loading control, actin proteins were immunodetected with an anti-Actin antibody.

BiFC and Split–LUC assays

In the BiFC assay with *N. benthamiana* plants, the eYFP fluorescence of expressed fusion proteins was recorded 2-3 days post infiltration with *A. tumefaciens* using a confocal microscope (Leica TCS SP8). For the Split–LUC assay, *N. benthamiana* leaves were collected at 2 days post infiltration and sprayed with a solution of 1 mM D-luciferin (Promega, E1603) and 0.02% (v/v) Triton X-100. After a dark adaptation of 5 min, bioluminescence images were acquired using a Tanon Bio–Imaging System (Tanon, Shanghai, 4600).

LC-MS analysis

For analysis of NopT phosphorylation sites, NopT-FLAG-His was co-expressed with His labelled NFR1^{CD} or NFR1$^{CD\text{-}K351E}$ in *E. coli*. The proteins were purified using Ni-charged resin (GenScript, Cat. No. L00223). The bands containing NopT^{P} and NopT (control) proteins, were cut out, destained by 50 mM triethylammonium bicarbonate (TEAB) solution (50% (v/v) acetonitrile in 50 mM TEAB), and washed with 100% acetonitrile until the gel turned white. The protein bands were then in-gel digested with sequencing-grade trypsin. LC-MS analysis was performed by Novogene Co., Ltd. (Beijing, China).

For identificaiton of the cleavage site in NFR5, NopT and His-SUMO-NFR5^{CD}-GST, were co-expressed in *E. coli* and purified using Glutathione Resin (GenScript, # L00206). About 80 μg of the cleaved protein was collected for analysis. The protein

bands were digested with trypsin,glu-C, chymotrypsin and pepsin. LC-MS analysis was performed by Oulu Biotechnology Co., Ltd. (Shanghai, China).

Examination of rhizobial infection

The morphology of rhizobial infection foci and infection threads have been described previously (Rae et al., 2021). In brief, an infection focus is formed when the tip of a root hair curls around a single bacterium, forming an infection pocket. The number of infection foci and infection threads was determined using a Leica fluorescence microscope (DM2500). Whole roots were mounted on microscope slides and infection foci and infection thread counts were expressed on a per-root basis.

Histochemical GUS staining of *L. japonicus* Gifu B-129 or Gifu *pNIN*:*GUS* roots inoculated with different rhizobial strains was performed using the chromogenic substrate 5-bromo-4-chloro-3-indolyl-β-D-glucuronide as described (Heckmann et al., 2011). After evacuation of air for 20 min, root samples were incubated in GUS staining solution overnight (at 37°C in the dark). The GUS-stained tissues were observed and photographed using a Motic Swift M200D compound microscope (Gifu B-129 roots inoculated with rhizobial strains harboring pT7-GUS) or a Nikon SMZ18 stereo microscope (Gifu *pNIN*:*GUS* inoculated with unlabeled rhizobia).

Supplemental data

Supplemental Fig. 1. Analyses of the functions of all 15 effectors from *S. fredii* NGR234 in preventing NFR1- and NFR5-induced cell death in *N. benthamiana* leaves.

Supplemental Fig. 2. Split–LUC assay testing the interactions between different NopT mutants and NFRs.

Supplemental Fig. 3. NopT cleaves NFR5 not not NFR1.

Supplemental Fig. 4. NopT interacts with the JM domain of NFR5.

Supplemental Fig. 5. Conserved domains and residues of NFR5 and related proteins.

Supplemental Fig. 6. NopT cleaves NFR5 at the juxtamembrane domain.

Supplemental Fig. 7. Mass spectrometry analysis of cleavage site of NFR5 by NopT.

Supplemental Fig. 8. NopT cleaves the NFR5 homolog proteins at the juxtamembrane domain.

Supplemental Fig. 9. NopT cleaves the JM of MtNFP.

Supplemental Fig. 10. NopT cleaves recombinant proteins $NFR5^{268-445}$-$NFP^{458-595}$ and $NFP^{270-457}$-$NFR^{5456-595}$.

Supplemental Fig. 11. $NFR1^{CD}$ phosphorylates $NFR5^{CD}$ *in vitro*.

Supplemental Fig. 12. Rhizobial infection in the mutant versions of NFR5.

Supplemental Fig. 13. Phylogenetic tree based on the amino acid sequence of NopT homologs from different bacterial species.

Supplemental Fig. 14. The cleavage efficiency of NFR5 in different system.

Supplemental Fig. 15. Transient expression of NopT triggers cell death in *Arabidopsis thaliana* and *Nicotiana tabacum***.**

Supplemental Table 1. Phosphopeptides of NopT identified by LC-MS.

Supplemental Table 2. Primers used in this study.

Acknowledgments: We greatly thank Prof. Zhongming Zhang for his valuable suggestions on this project. We thank Drs. Eric Giraud, Ertao Wang, and Yan Liang for critical reading of this manuscript. We thank Dr. Jens Stougaard for kindly providing *L. japonicus pNIN:GUS* and *nfr* mutant seeds. Dr. Juan Du is thanked for providing plasmids for expression of Avr3a and R3a, BAX, and INF1. The qPCR and microscopy data were acquired from the Core Facility Center at the National Key Lab of Agricultural Microbiology.

Funding: This work was supported by the National Key R&D Program of China (2019YFA0904700), the National Natural Science Foundation of China (32090063), and the Fundamental Research Funds for the Central Universities (2662022SKYJ002 and 2662021JC010). Work in the Stacey's lab was supported by the NSF Plant Genome Research Program (2048410)..

Author Contributions: H.B., Y.C., and G.S. conceived the idea and designed the research, H.B., Y.W., Y.L., and Y.Y. performed experiments; H.B., Y.W., H. L., H.Z., and Y.C. analyzed the data; Q.W. and S.X. identified the cleavage site by MS. H.B., Y.C., S.F.W., C.S., and G.S. wrote the paper.

References

Akeda, Y., and Galán, J.E. (2005). Chaperone release and unfolding of substrates in type III secretion. Nature **437,** 911-915.

Bos, J.I., Kanneganti, T.D., Young, C., Cakir, C., Huitema, E., Win, J., Armstrong, M.R., Birch, P.R., and Kamoun, S. (2006). The C-terminal half of *Phytophthora infestans* RXLR effector AVR3a is sufficient to trigger R3a-mediated hypersensitivity and suppress INF1-induced cell death in *Nicotiana benthamiana*. Plant J **48,** 165-176.

Bozsoki, Z., Cheng, J., Feng, F., Gysel, K., Vinther, M., Andersen, K.R., Oldroyd, G., Blaise, M., Radutoiu, S., and Stougaard, J. (2017). Receptor-mediated chitin perception in legume roots is functionally separable from Nod factor perception. Proc Natl Acad Sci U S A **114,** E8118-E8127.

Broghammer, A., Krusell, L., Blaise, M., Sauer, J., Sullivan, J.T., Maolanon, N., Vinther, M., Lorentzen, A., Madsen, E.B., Jensen, K.J., Roepstorff, P., Thirup, S., Ronson, C.W., Thygesen, M.B., and Stougaard, J. (2012). Legume receptors perceive the rhizobial lipochitin oligosaccharide signal molecules by direct binding. Proc Natl Acad Sci U S A **109,** 13859-13864.

Cao, Y., Liang, Y., Tanaka, K., Nguyen, C.T., Jedrzejczak, R.P., Joachimiak, A., and Stacey, G. (2014). The kinase LYK5 is a major chitin receptor in *Arabidopsis* and forms a chitin-induced complex with related kinase CERK1. eLife **3**.e03766.

Cai J, Zhang LY, Liu W, Tian Y, Xiong JS, Wang YH, Li RJ, Li HM, Wen J, Mysore KS, Boller T, Xie ZP, Staehelin C. (2018). Role of the Nod factor hydrolase MtNFH1 in regulating Nod factor levels during rhizobial infection and in mature nodules of *Medicago truncatula*. Plant Cell **30,** 397-414.

Dai, W.J., Zeng, Y., Xie, Z.P., and Staehelin, C. (2008). Symbiosis-promoting and deleterious effects of NopT, a novel type 3 effector of *Rhizobium* sp. strain NGR234. J Bacteriol **190,** 5101-5110.

Dowen, R.H., Engel, J.L., Shao, F., Ecker, J.R., and Dixon, J.E. (2009). A family of bacterial cysteine protease type III effectors utilizes acylation-dependent and

-independent strategies to localize to plasma membranes. J Biol Chem **284,** 15867-15879.

Fotiadis, C.T., Dimou, M., Georgakopoulos, D.G., Katinakis, P., and Tampakaki, A.P. (2012). Functional characterization of NopT1 and NopT2, two type III effectors of *Bradyrhizobium japonicum*. FEMS Microbiol Lett **327,** 66-77.

Gan, Y., Zhang, L., Zhang, Z., Dong, S., Li, J., Wang, Y., and Zheng, X. (2009). The LCB2 subunit of the sphingolip biosynthesis enzyme serine palmitoyltransferase can function as an attenuator of the hypersensitive response and Bax-induced cell death. New Phytol **181,** 127-146.

Geurts, R., Fedorova, E., and Bisseling, T. (2005). Nod factor signaling genes and their function in the early stages of infection. Curr Opin Plant Biol **8,** 346-352.

Goehre, V., Spallek, T., Haeweker, H., Mersmann, S., Mentzel, T., Boller, T., de Torres, M., Mansfield, J.W., and Robatzek, S. (2008). Plant pattern-recognition receptor FLS2 is directed for degradation by the bacterial ubiquitin ligase AvrPtoB. Curr Biol **18,** 1824-1832.

Gysel, K., Laursen, M., Thygesen, M.B., Lironi, D., Bozsoki, Z., Hjuler, C.T., Maolanon, N.N., Cheng, J., Bjork, P.K., Vinther, M., Madsen, L.H., Rubsam, H., Muszynski, A., Ghodrati, A., Azadi, P., Sullivan, J.T., Ronson, C.W., Jensen, K.J., Blaise, M., Radutoiu, S., Stougaard, J., and Andersen, K.R. (2021). Kinetic proofreading of lipochitooligosaccharides determines signal activation of symbiotic plant receptors. Proc Natl Acad Sci U S A **118**.e2111031118.

Han, Y., Sun, J., Yang, J., Tan, Z., Luo, J., and Lu, D. (2017). Reconstitution of the plant ubiquitination cascade in bacteria using a synthetic biology approach. Plant J **91,** 766-776.

Heckmann, A.B., Sandal, N., Bek, A.S., Madsen, L.H., Jurkiewicz, A., Nielsen, M.W., Tirichine, L., and Stougaard, J. (2011). Cytokinin induction of root nodule primordia in *Lotus japonicus* is regulated by a mechanism operating in the root cortex. Mol Plant Microbe Interact **24,** 1385-1395.

Jones, J.D.G., and Dangl, J.L. (2006). The plant immune system. Nature **444,** 323-329.

Kambara, K., Ardissone, S., Kobayashi, H., Saad, M.M., Schumpp, O., Broughton, W.J., Deakin W.J. (2009). Rhizobia utilize pathogen-like effector proteins during symbiosis. Mol Microbiol **71,** 92-106.

Kawaharada, Y., Kelly, S., Nielsen, M.W., Hjuler, C.T., Gysel, K., Muszynski, A., Carlson, R.W., Thygesen, M.B., Sandal, N., Asmussen, M.H., Vinther, M., Andersen, S.U., Krusell, L., Thirup, S., Jensen, K.J., Ronson, C.W., Blaise, M., Radutoiu, S., and Stougaard, J. (2015). Receptor-mediated exopolysaccharide perception controls bacterial infection. Nature **523,** 308-312.

Kato, Y., and Sakamoto, W. (2019). Phosphorylation of the chloroplastic metalloprotease FtsH in Arabidopsis characterized by Phos-tag SDS-PAGE. Front Plant Sci, 10, 1080.

Khan, A., Wadood, S.F., Chen, M., Wang, Y., Xie, Z.P., and Staehelin, C. (2022). Effector-triggered inhibition of nodulation: A rhizobial effector protease targets soybean kinase GmPBS1-1. Plant Physiol **189,** 2382-2395.

Kim, S.H., Qi, D., Ashfield, T., Helm, M., and Innes, R.W. (2016). Using decoys to expand the recognition specificity of a plant disease resistance protein. Science **351,** 684-687.

Kimbrel, J.A., Thomas, W.J., Jiang, Y., Creason, A.L., Thireault, C.A., Sachs, J.L., and Chang, J.H. (2013). Mutualistic co-evolution of type III effector genes in Sinorhizobium fredii and *Bradyrhizobium japonicum*. PLoS Pathog **9,** e1003204.

Kopan, R., and Ilagan, M.X.G. (2009). The canonical notch signaling pathway: Unfolding the activation mechanism. Cell **137,** 216-233.

Lei, L., Stevens, D.M., and Coaker, G. (2020). Phosphorylation of the *Pseudomonas* effector AvrPtoB by *Arabidopsis* SnRK2.8 is required for bacterial virulence. Mol Plant **13,** 1513-1522.

Li, D.D., Zhu, Z.K., Deng, X.M., Zou, J.N., Ma, C., Li, C.D., Yin, T., Liu, C.Y., Wang, J.H., Chen, Q.S., and Xin, D.W. (2023). GmPBS1, a hub gene interacting with rhizobial type-III effectors NopT and NopP, regulates soybean nodulation. Agronomy **13,** 1242.

Li, H., Chen, M., Duan, L., Zhang, T., Cao, Y., and Zhang, Z. (2018). Domain swap approach reveals the critical roles of different domains of SYMRK in root nodule symbiosis in *Lotus japonicus*. Front Plant Sci **9,** 697.

Li, L., Kim, P., Yu, L., Cai, G., Chen, S., Alfano, J.R., and Zhou, J.M. (2016). Activation-dependent destruction of a co-receptor by a *Pseudomonas syringae* effector dampens plant immunity. Cell Host Microbe **20,** 504-514.

Luo, Y., Liu, D., Jiao, S., Liu, S., Wang, X., Shen, X., and Wei, G. (2020) Identification of *Robinia pseudoacacia* target proteins responsive to *Mesorhizobium amphore* CCNWGS0123 effector protein NopT. J Exp Bot. **71,** 7347-7363.

Madsen, E.B., Madsen, L.H., Radutoiu, S., Olbryt, M., Rakwalska, M., Szczyglowski, K., Sato, S., Kaneko, T., Tabata, S., Sandal, N., and Stougaard, J. (2003). A receptor kinase gene of the LysM type is involved in legume perception of rhizobial signals. Nature **425,** 637-640.

Madsen, E.B., Antolin-Llovera, M., Grossmann, C., Ye, J., Vieweg, S., Broghammer, A., Krusell, L., Radutoiu, S., Jensen, O.N., Stougaard, J., and Parniske, M. (2011). Autophosphorylation is essential for the *in vivo* function of the *Lotus japonicus* Nod factor receptor 1 and receptor-mediated signalling in cooperation with Nod factor receptor 5. Plant J **65,** 404-417.

Moling, S., Pietraszewska-Bogiel, A., Postma, M., Fedorova, E., Hink, M.A., Limpens, E., Gadella, T.W., and Bisseling, T. (2014). Nod factor receptors form heteromeric complexes and are essential for intracellular infection in *Medicago* nodules. Plant Cell **26,** 4188-4199.

Nakagawa, T., Suzuki, T., Murata, S., Nakamura, S., Hino, T., Maeo, K., Tabata, R., Kawai, T., Tanaka, K., Niwa, Y., Watanabe, Y., Nakamura, K., Kimura, T., and Ishiguro, S. (2007). Improved Gateway binary vectors: high-performance vectors for creation of fusion constructs in transgenic analysis of plants. Biosci Biotechnol Biochem **71,** 2095-2100.

Ntoukakis, V., Mucyn, T.S., Gimenez-Ibanez, S., Chapman, H.C., Gutierrez, J.R., Balmuth, A.L., Jones, A.M., and Rathjen, J.P. (2009). Host inhibition of a bacterial virulence effector triggers immunity to infection. Science **324,** 784-787.

Radutoiu S, Madsen LH, Madsen EB, Felle HH, Umehara Y, Grønlund M, Sato S, Nakamura Y, Tabata S, Sandal N, Stougaard J. (2003). Plant recognition of symbiotic bacteria requires two LysM receptor-like kinases. Nature **425,** 585-592.

Rae, A.E., Rolland, V., White, R.G., and Mathesius, U. (2021). New methods for confocal imaging of infection threads in crop and model legumes. Plant Methods **17**, 24.

Ried, MK, Antolín-Llovera, M, and Parniske, M. (2014). Spontaneous symbiotic reprogramming of plant roots triggered by receptor-like kinases. Elife **3,** e03891.

Schauser, L., Roussis, A., Stiller, J., and Stougaard J. (1999) A plant regulator controlling development of symbiotic root nodules. Nature **402,** 191-195.

Schmidt, G. (2011). *Yersinia enterocolitica* outer protein T (YopT). Eur J Cell Biol **90,** 955-958.

Schubert, K.A., Xu, Y., Shao, F., and Auerbuch, V. (2020). The type III secretion system as a tool for studying cytosolic innate immune surveillance. Ann Rev Microbiol, Vol 74, 2020 **74,** 221-245.

Shao, F., Merritt, P.M., Bao, Z., Innes, R.W., and Dixon, J.E. (2002). A *Yersinia* effector and a *Pseudomonas* avirulence protein define a family of cysteine proteases functioning in bacterial pathogenesis. Cell **109,** 575-588.

Shao, F., Vacratsis, P.O., Bao, Z., Bowers, K.E., Fierke, C.A., and Dixon, J.E. (2003a). Biochemical characterization of the *Yersinia* YopT protease: cleavage site and recognition elements in Rho GTPases. Proc Natl Acad Sci U S A **100,** 904-909.

Shao, F., Golstein, C., Ade, J., Stoutemyer, M., Dixon, J.E., and Innes, R.W. (2003b). Cleavage of *Arabidopsis* PBS1 by a bacterial type III effector. Science **301,** 1230-1233.

Sugawara, M., Takahashi, S., Umehara, Y., Iwano, H., Tsurumaru, H., Odake, H., Suzuki, Y., Kondo, H., Konno, Y., Yamakawa, T., Sato, S., Mitsui, H., and Minamisawa, K. (2018). Variation in bradyrhizobial NopP effector determines symbiotic incompatibility with soybeans via effector-triggered immunity. Nature Commun **9**.3139.

Sun, Y., Li, L., Macho, A.P., Han, Z., Hu, Z., Zipfel, C., Zhou, J.-M., and Chai, J. (2013). Structural basis for flg22-induced activation of the *Arabidopsis* FLS2-BAK1 immune complex. Science **342,** 624-628.

Tang, D.Z., Wang, G.X., and Zhou, J.M. (2017). Receptor kinases in plant-pathogen interactions: More than pattern recognition. Plant Cell **29,** 618-637.

Teulet, A., Busset, N., Fardoux, J., Gully, D., Chaintreuil, C., Cartieaux, F., Jauneau, A., Comorge, V., Okazaki, S., Kaneko, T., Gressent, F., Nouwen, N., Arrighi, J.F., Koebnik, R., Mergaert, P., Deslandes, L., and Giraud, E. (2019). The rhizobial type III effector ErnA confers the ability to form nodules in legumes. Proc Natl Acad Sci U S A **116,** 21758-21768.

Tirichine, L., Imaizumi-Anraku, H., Yoshida, S., Murakami, Y., Madsen, L.H., Miwa, H., Nakagawa, T., Sandal, N., Albrektsen, A.S., Kawaguchi, M., Downie, A., Sato, S., Tabata, S., Kouchi, H., Parniske, M., Kawasaki, S., and Stougaard, J. (2006). Deregulation of a Ca2+/calmodulin-dependent kinase leads to spontaneous nodule development. Nature **441,** 1153-1156.

Vleeshouwers, V.G., Driesprong, J.D., Kamphuis, L.G., Torto-Alalibo, T., Van't Slot, K.A., Govers, F., Visser, R.G., Jacobsen, E., and Kamoun, S. (2006). Agroinfection-based high-throughput screening reveals specific recognition of INF elicitins in *Solanum*. Mol Plant Pathol **7,** 499-510.

Wang, D., Yang, S., Tang, F., and Zhu, H. (2012). Symbiosis specificity in the legume: rhizobial mutualism. Cell Microbiol **14,** 334-342.

Wang, Q., Han, C., Ferreira, A.O., Yu, X., Ye, W., Tripathy, S., Kale, S.D., Gu, B., Sheng, Y., Sui, Y., Wang, X., Zhang, Z., Cheng, B., Dong, S., Shan, W., Zheng, X., Dou, D., Tyler, B.M., and Wang, Y. (2011). Transcriptional programming and functional interactions within the *Phytophthora sojae* RXLR effector repertoire. Plant Cell **23,** 2064-2086.

Xiang, T., Zong, N., Zou, Y., Wu, Y., Zhang, J., Xing, W., Li, Y., Tang, X., Zhu, L., Chai, J., and Zhou, J.M. (2008). *Pseudomonas syringae* effector AvrPto blocks innate immunity by targeting receptor kinases. Curr Biol **18,** 74-80.

Xin, D.W., Liao, S., Xie, Z.P., Hann, D.R., Steinle, L., Boller, T., Staehelin, C. (2012). Functional analysis of NopM, a novel E3 ubiquitin ligase (NEL) domain effector of *Rhizobium* sp. strain NGR234. PLoS Pathog **8(5),** e1002707.

Xu, N., Luo, X., Wu, W., Xing, Y., Liang, Y., Liu, Y., Zou, H., Wei, H.L., and Liu, J. (2020). A plant lectin receptor-like kinase phosphorylates the bacterial effector AvrPtoB to dampen lits virulence in *Arabidopsis*. Mol Plant **13,** 1499-1512.

Yang, J., Lan, L., Jin, Y., Yu, N., Wang, D., and Wang, E. (2022). Mechanisms underlying legume-rhizobium symbioses. J Integr Plant Biol **64,** 244-267.

Zhang, B., Wang, M., Sun, Y., Zhao, P., Liu, C., Qing, K., Hu, X., Zhong, Z., Cheng, J., Wang, H., Peng, Y., Shi, J., Zhuang, L., Du, S., He, M., Wu, H., Liu, M., Chen, S., Wang, H., Chen, X., Fan, W., Tian, K., Wang, Y., Chen, Q., Wang, S., Dong, F., Yang, C., Zhang, M., Song, Q., Li, Y., and Wang, X. (2021). *Glycine max* NNL1 restricts symbiotic compatibility with widely distributed *Bradyrhizobia vi*a root hair infection. Nat Plants **7,** 73-86.

Zhang, J., Li, W., Xiang, T., Liu, Z., Laluk, K., Ding, X., Zou, Y., Gao, M., Zhang, X., Chen, S., Mengiste, T., Zhang, Y., and Zhou, J.M. (2010). Receptor-like cytoplasmic kinases integrate signaling from multiple plant immune receptors and are targeted by a *Pseudomonas syringae* effector. Cell Host Microbe **7,** 290-301.

Zhou, J.G., Wang, P., Claus, L.A.N., Savatin, D.V., Xu, G.Y., Wu, S.J., Meng, X.Z., Russinova, E., He, P., and Shan, L.B. (2019). Proteolytic processing of SERK3/BAK1 regulates plant immunity, development, and cell death. Plant Physiol **180,** 543-558.

Zipfel, C., and Oldroyd, G.E.D. (2017). Plant signalling in symbiosis and immunity. Nature **543,** 328-336.

Zipfel, C., Robatzek, S., Navarro, L., Oakeley, E.J., Jones, J.D.G., Felix, G., and Boller, T. (2004). Bacterial disease resistance in through flagellin perception. Nature **428,** 764-767.

Figures

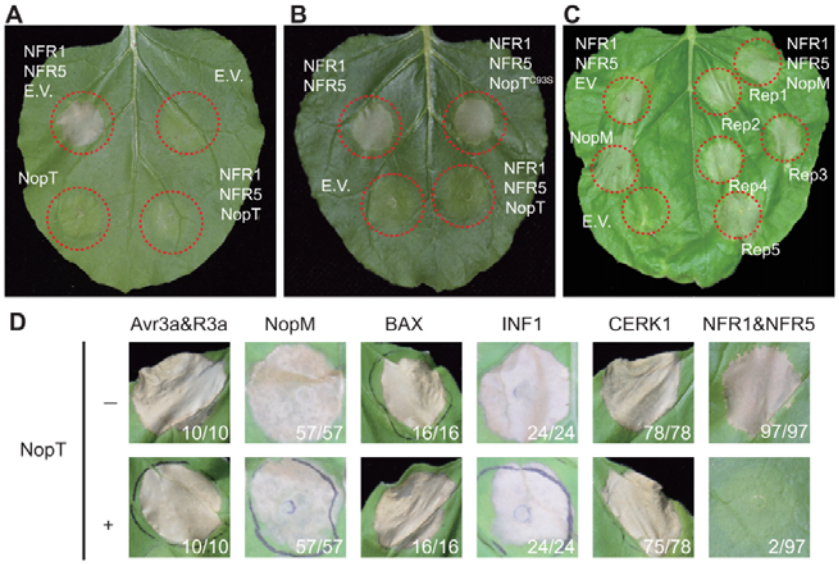

Figure 1. NopT specifically suppresses NFR1/NFR5-triggered cell death in *N. benthamiana*. *Agrobacterium* strains harboring plasmid DNA encoding NopT or the empty vector (EV) were infiltrated into *N. benthamiana* leaves. At 12 hpi, a second infiltration was performed with an *Agrobacterium* strain containing a plasmid with *NFR1*/*NFR5* genes. Dashed red lines indicate leaf discs where different proteins were expressed. (A, B) NopT (A), but not NopT^{C93S} (B), a protease-inactive version of NopT, suppressed NFR1NFR5-induced cell death. (C) Expression of NopM-induced cell death in *N. benthamiana*. (D) Expression of NopT could not suppress the cell death response triggered by expression of Avr3a/R3a, NopM, BAX, INF1 or AtCERK1. Numbers in (D) represent the number of leaf discs showing cell death and total leaf discs tested. The pictures shown in this figure are representative of at least three independent biological replicates.

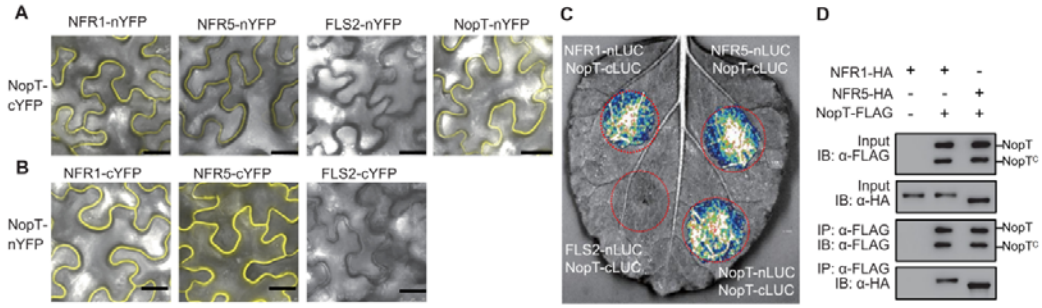

Figure 2. NopT interacts with NFR1 and NFR5. Interactions between NopT and NFR1 or NFR5 were detected using BiFC (Split-YFP) (A, B), Split-LUC complementation (C) and co-IP (D) assays in *N. benthamiana* leaves. (A, B) For BIFC analysis, nYFP and cYFP tags were fused at the C-terminus of NopT, NFR1, NFR5, and the flagellin receptor FLS2 (negative control). YFP fluorescence signals represent protein-protein interactions. Scale bar=25 μm. (C) For the Split-LUC complementation assay, the nLUC and cLUC tags were fused at the C-terminus of NopT, NFR1, NFR5 and FLS2 (negative control). Luminescence signals represent protein-protein interactions. (D) For the co-IP assay, HA-tagged NFR1 or NFR5 and FLAG-tagged NopT were expressed in *N. benthamiana* cells followed by immunoprecipitation using an anti-FLAG antibody. Immunoblot analysis was performed using anti-HA and anti-FLAG antibodies ($NopT^C$ denotes the truncated version of NopT after autocleavage). The images and immunoblots shown in this figure are representative of three biological replicates.

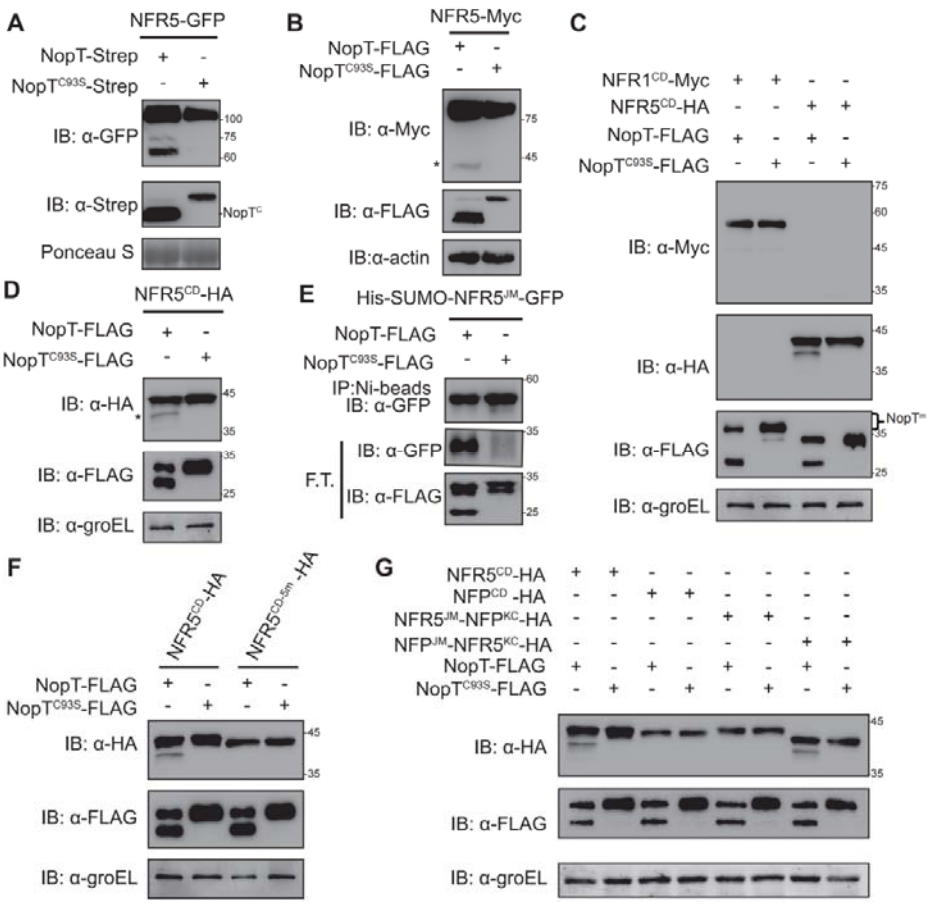

Figure 3. NopT proteolyzes NFR5 at its JM domain. Proteins with indicated tags were expressed in *N. benthamiana* (A), *L. japonicus* (B) or *E. coli* (C-G) and detected by immunoblotting. (A) NopT but not NopT^{C93S} cleaves NFR5-GFP protein expressed in *N. benthamiana* cells by releasing NFR5^{CD}-GFP (NopT^{C} denotes autocleaved NopT). (B) NopT but not NopT^{C93S} cleaves NFR5-Myc expressed in hairy roots of *L. japonicus* by releasing NFR5^{CD}-Myc (marked by an asterisk). (C) Analysis of the CDs of NFR1 and NFR5 co-expressed with NopT or NopT^{C93S} in *E. coli*. Cleavage of NFR5^{CD} was observed for NopT but not NopT^{C93S}, while NFR1^{CD} was not proteolyzed by NopT. In the presence of NFR1^{CD}, a slower migrating band was observed, possibly representing phosphorylated NopT (NopT^{m}). (D) A repeat experiment confirmed that NopT is able to cleave NFR5^{CD} (the asterisk indicates the HA-tagged NFR5 cleavage product containing the kinase domain and a C-terminal tail region). (E) NopT cleaves His-SUMO-NFR5^{JM}-GFP (His-SUMO and GFP linked by the JM

domain of NFR5) *in vitro*. F.T. indicates proteins in flow through samples after purification with Ni-beads. (F) NopT expressed in *E. coli* was unable to cleave co-expressed NFR5$^{CD\text{-}5m}$-HA, a modified version of NFR5^{CD}-HA in which five amino acids of the JM were substituted by other residues (S283Y, G294Q, Y303S, A310I, T311Y). (G) NopT expressed in *E. coli* was unable to cleave co-expressed *M. truncatula* NFP^{CD}-HA and the NFR5^{JM}-NFP^{KC}-HA fusion protein, while NFP^{JM}-NFR5^{KC} was proteolyzed (KC stands for the kinase domain and a C-terminal tail region).

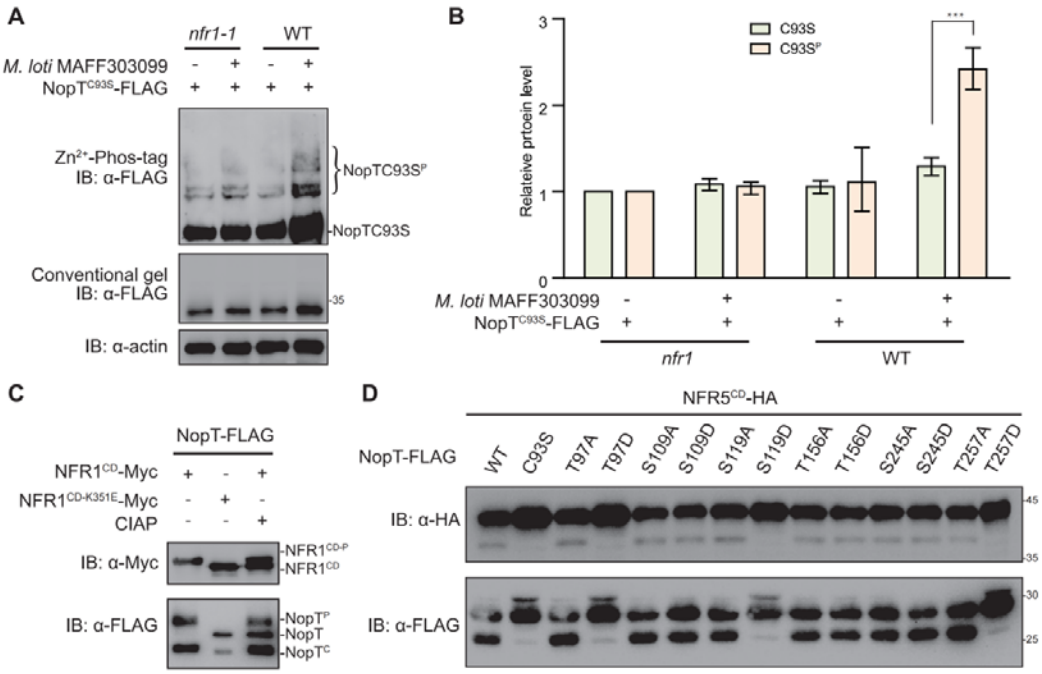

Figure 4. Phosphorylation of NopT by NFR1 suppresses its proteolytic activity. (A) *In vivo* phosphorylation assay with proteins expressed in *L. japonicus* roots (wild-type and *nfr1-1* mutant plants) using Zn^{2+}-Phos-tag SDS-PAGE. Phosphorylation of $NopT^{C93S}$ was induced by inoculation with rhizobia (*Mesorhizobium loti* MAFF303099) and was largely dependent on *NFR1*. (B) The relative protein amount of each lane, as shown in (A), was quantified with ImageJ software (three biological replicates). The value of the control band in each gel was set to 1 for comparison. Values are means ± SEM. (C) $NFR1^{CD}$ but not $NFR1^{CD\text{-}K351E}$ phosphorylates NopT in *E. coli*. The phosphorylated full-length form of NopT could be dephosphorylated by CIAP (gel band shift). Abbreviations: $NFR1^{CD\text{-}P}$, autophosphorylated NFR1; $NopT^{P}$, phosphorylated NopT; NopT, non-phosphorylated NopT; $NopT^{C}$, autocleaved NopT. (D) The phoshorylation sites of NopT identified by LC-MS were either substituted to alanine (A) or aspartate (D). The indicated NopT variants were subsequently tested for autocleavage and $NFR5^{CD}$ proteolysis in *E. coli*. Wild-type NopT (WT) and protease-dead $NopT^{C93S}$ were included into the analysis.

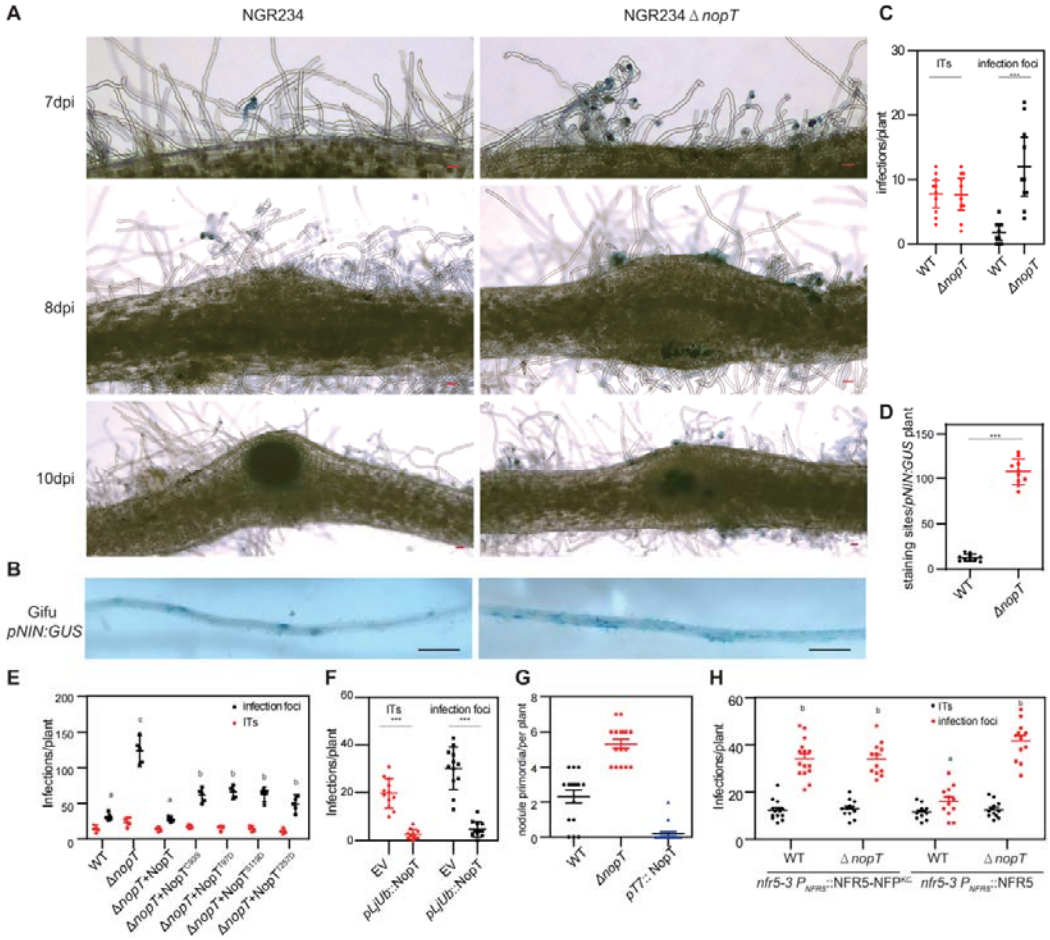

Figure 5. NopT regulates rhizobial infection in *L. japonicus*. (A) Analysis of rhizobial infection in *L. japonicus* roots inoculated with *GUS*-labelled *S. fredii* NGR234 (wild-type; WT) or a *nopT* knockout mutant (NGR234Δ*nopT*; abbreviated as Δ*nopT* in other panels). Scale bar=100 µm. (B) GUS staining pictures showing roots of *L. japonicus* plants expressing *GUS* expression under control of the *NIN* promoter (*pNIN*:*GUS*). Plants were inoculated with NGR234 or NGR234Δ*nopT* and analyzed at 7 dpi. Scale bar=1 mm. (C) Infection data (ITs, infection threads) for roots shown in (A) at 7 dpi (n=10, Student's *t*-test; * indicates P < 0.01). (D) Quantification of GUS staining sites for roots shown in (B) (n=10, Student's *t*-test, P < 0.01). (E) Nodule primordia formation in *L. japonicus* wild-type roots inoculated with NGR234 (WT), NGR234Δ*nopT* or NGR234 over-expressing *nopT* (*pT7*:NopT). Roots were analyzed at 14 dpi (n=16, Student's *t*-test: P < 0.01). (F) Infection data for wild-type roots inoculated with NGR234 (WT), NGR234Δ*nopT* and NGR234Δ*nopT* expressing indicated NopT variants at 7 dpi (n=5, Student's *t*-test: P < 0.01). (G) Analysis of

rhizobial infection in hairy roots of *L. japonicus* (wild-type) expressing GFP (EV, empty vector control) or NopT. Plants were inoculated with DsRed-labeled *M. loti* MAFF303099 and analyzed at 5 dpi (n=8, Student's t–test: $P < 0.01$). (H) Expression of NFR5 and NFR5-NFP^{KC} in hairy roots of *nfr5-3* mutant plants. Plants were inoculated with GFP-labelled NGR234 (WT) or NGR234Δ*nopT* and analyzed at 8 dpi . Roots expressing NFR5-NFP^{KC} showed high numbers of infection foci for both strains whereas significant differences were observed for NFR5 expressing roots (n=10, Student's t-test: $P < 0.01$).

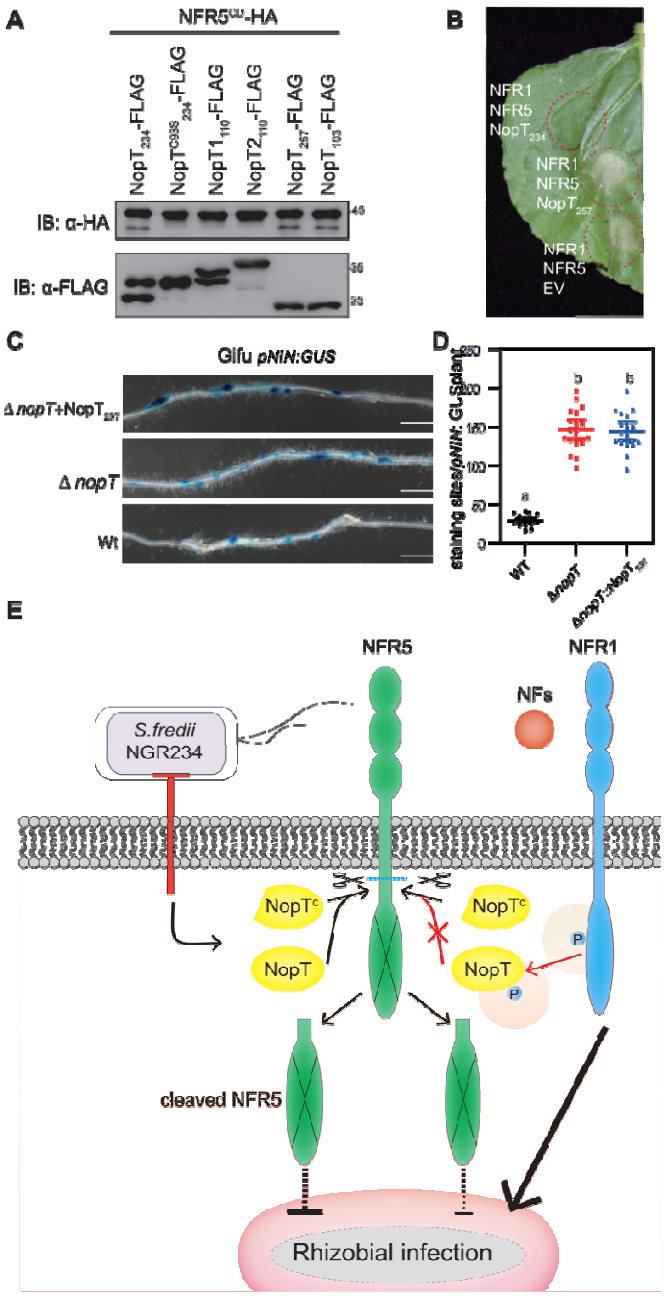

Figure 6. *S. fredii* NopT proteins cleave NFR5 and working model for NopT of NGR234. (A) NopT of *S. fredii* NGR234 and homologs from other rhizobial strains were co-expressed with $NFR5^{CD}$ in *E. coli* ($NopT_{234}$, NopT of NGR234; $NopT1_{110}$ and $NopT2_{110}$, NopT proteins of *B. diazoefficiens* USDA110; $NopT_{257}$, NopT of *S. fredii* USDA257; $NopT_{103}$, NopT of *S. fredii* HH103). Immunoblot analysis indicated NFR5 cleavage by NopT proteins from *S. fredii*

strains. (B) Expression of $NopT_{257}$ in *N. benthamiana* could not inhibit the cell death triggered by co-expressed NFR1 and NFR5. (C) *L. japonicus* Gifu *pNIN*:*GUS* plants were inoculated with *S. fredii* NGR234, NGR234Δ*nopT* and NGR234Δ*nopT* expressing $NopT_{257}$ (Δ*nopT*+$NopT_{257}$). Roots were subjected to GUS staining at 7 dpi. Scale bar=2.5 mm. (D) Quantitative analysis of GUS-stained roots shown in panel C (n=19, Student's *t*–test: $P < 0.01$). (E) A proposed model for NopT of NGR234 interacting with NFRs. NopT and $NopT^C$ (autocleaved NopT) proteolytically cleave NFR5 at the JM domain to release the intracellular domain of NFR5 (cleaved NFR5). NFR1 phosphorylates full-length NopT to block its proteinase activity. $NopT^C$ cannot be phosphorylated by NFR1.

Supplemental Figures

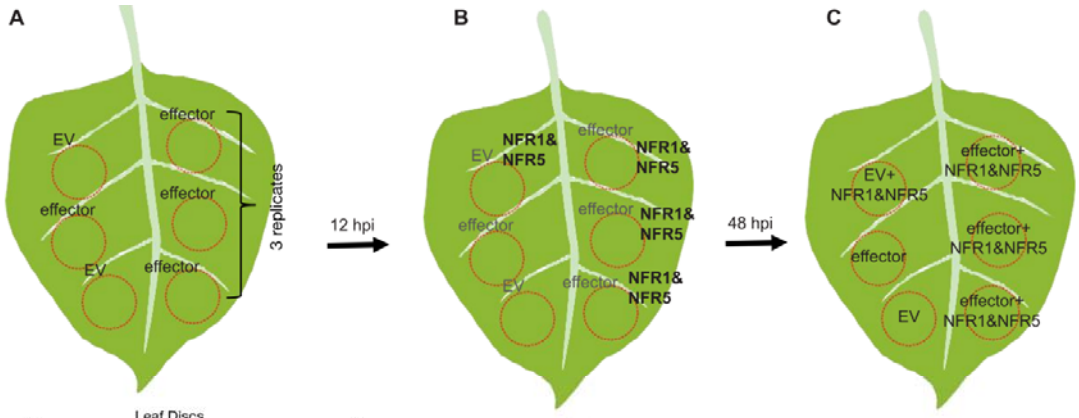

D

Effector	Leaf Discs (Cell death/total) Ctrl.	NFR1&NFR5
NopA	0/3	9/9
NopB	0/3	9/9
NopC	0/3	9/9
NopJ	0/3	9/9
NopL	0/3	9/9
NopM	3/3	9/9
NopP	0/3	9/9
NopT	0/3	0/9
NopU	0/3	9/9
NopV	0/3	9/9
NopX	0/3	9/9
NopY	0/3	9/9
NopZ	0/3	4/9
NopBE	0/3	9/9
NopBI	0/3	9/9

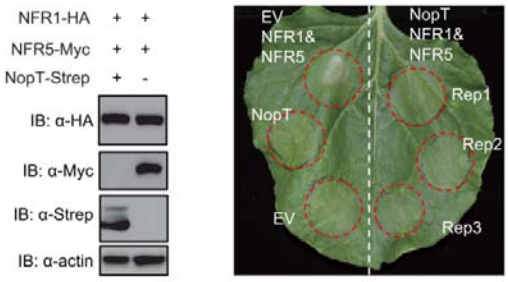

Supplemental Fig. 1. Analyses of the functions of all 15 effectors from *S. fredii* NGR234 in preventing NFR1- and NFR5-induced cell death in *N. benthamiana* leaves.

15 genes from *S. fredii* NGR234 encoding effector proteins were amplified and cloned into binary vector for expression of Strep-tagged proteins in *N. benthamiana*. NFR1 and NFR5 from *L. japonicus* were C-terminally tagged with HA and Myc, respectively, and cloned into binary vectors for expression in *N. benthamiana*. All plasmids were electroporated into *Agrobacterium tumefaciens* EH105.

(A) *Agrobacterium* strain harboring each effector gene or control empty vector (EV) were infiltrated into *N. benthamiana*. 12 hour post infiltration (hpi), agrobacterium strains harboring NFR1 and NFR5 were mixed and hand-infiltrated in the same leaf discs as shown in (B). 48 hpi, cell death phenotypes were evaluated (C). At least three replicates in the same leaf were

performed to test the function of each effector in suppressing cell death-triggered by NFR1 and LjNFR5. (D) Results of all 15 effector proteins in suppressing programmed cell death by overexpression of NFR1 and NFR5. (E) Abundance of NFR1, NFR5, and NopT proteins, as measured by immunoblot with specific antibodies. Leaf discs expressing NFR1, NFR5, and NopT or NFR1 and NFR5 and with EV were used for immunoblot analyses. Actin was used as loading control. (F) Another example of suppression of programmed cell death by NopT in the leaf discs coexpressing NFR1 and NFR5. Rep1, Rep2, and Rep3 represent three technical repeats in the same leave.

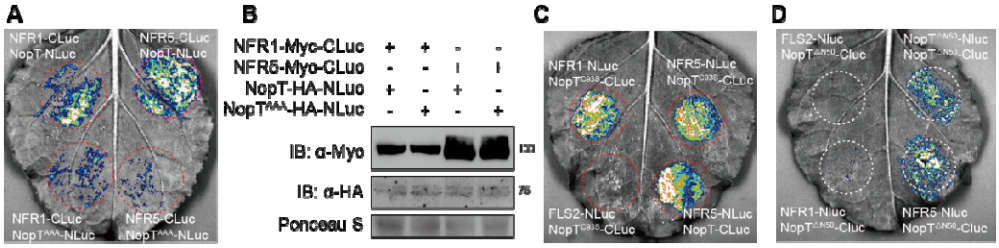

Supplemental Fig. 2. Split–LUC assay testing the interactions between different NopT mutants and NFRs.

(A)The interaction between NopT with mutated acylation site and NFR1/NFR5. $NopT^{AAA}$ (G50A, C51A, and C52A). (B) The protein expressing of indicating genes in the leave of (A). (C) Nop^{C93S} interact with NFR1 and NFR5. (D) The interaction between $NopT^{\Delta N50}$ and NFR5. $NopT^{\Delta N50}$ represents a truncated NopT with deletion of about 50 a.a. from its N–terminus.

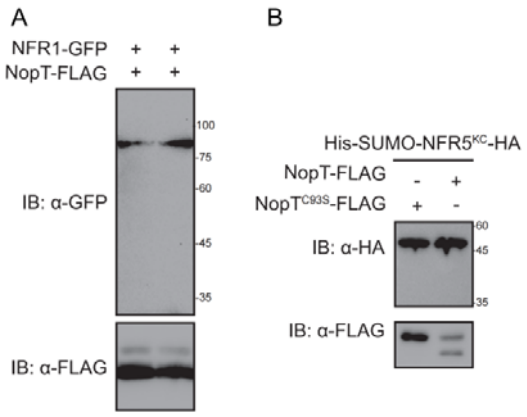

Supplemental Fig. 3. NopT cleaves NFR5 not not NFR1.

Proteins with indicated tags were expressed in either *N. benthamiana* or *E. coli* and detected by immunoblotting. (A) NopT did not cleave NFR1-GFP expressed in *N. benthamiana* leaves. (B) NopT expressed in *E. coli* did not cleave co-expressed SUMO-NFR5^{KC}-HA. KC: Kinase domain and C-terminal domain

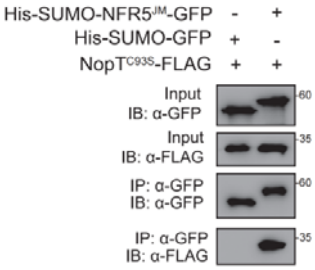

Supplemental Fig. 4. NopT interacts with the JM domain of NFR5.

NopT interacts with NFR5^{JM} in *in vitro* pull down assay. IB: immunoblotting, IP: immunoprecipitation. His-SUMO-NFR5^{JM}-GFP: a recombinant protein containing His tag, SUMO tag, the JM domain of NFR5, and GFP.

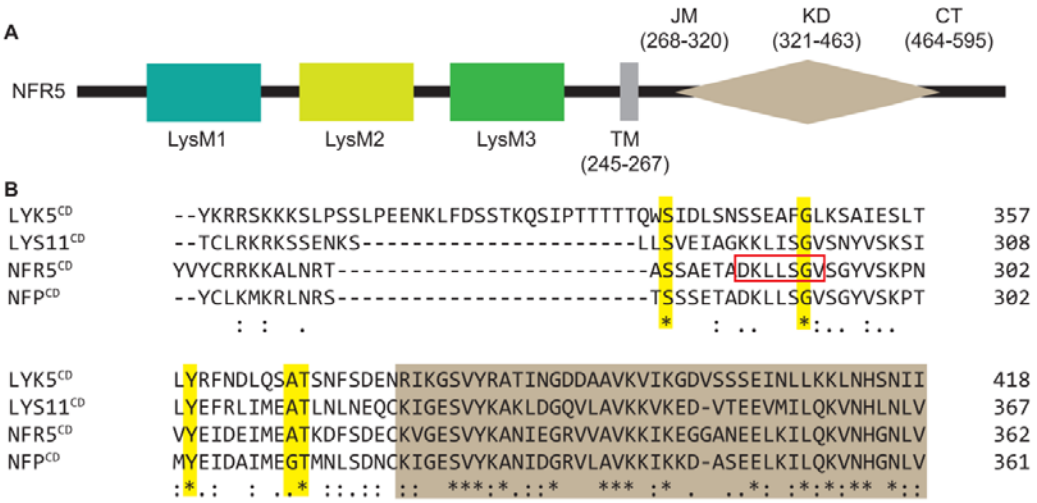

Supplemental Fig. 5. Conserved domains and residues of NFR5 and related proteins.

(A) Domain and motif annotation of NFR5. LysM: Lysin-Motif; TM: transmembrane domain; JM: juxtamembrane domain; KD: kinase domain; CT: C-terminal domain. (B) Alignment of amino acid residues of AtLYK5, LjLYS11, NFR5 and MtNFP close to the RRKK motif in the JM domain of NFR5. Five highly conserved residues marked by yellow coloration (S283, G294, Y304, A310, T311 in NFR5) and the brown box indicates the start region of kinase domain. The green frame delineates the RRKK motif in NFR5 and the red-framed residues are similar to the NopT autocleavage region.

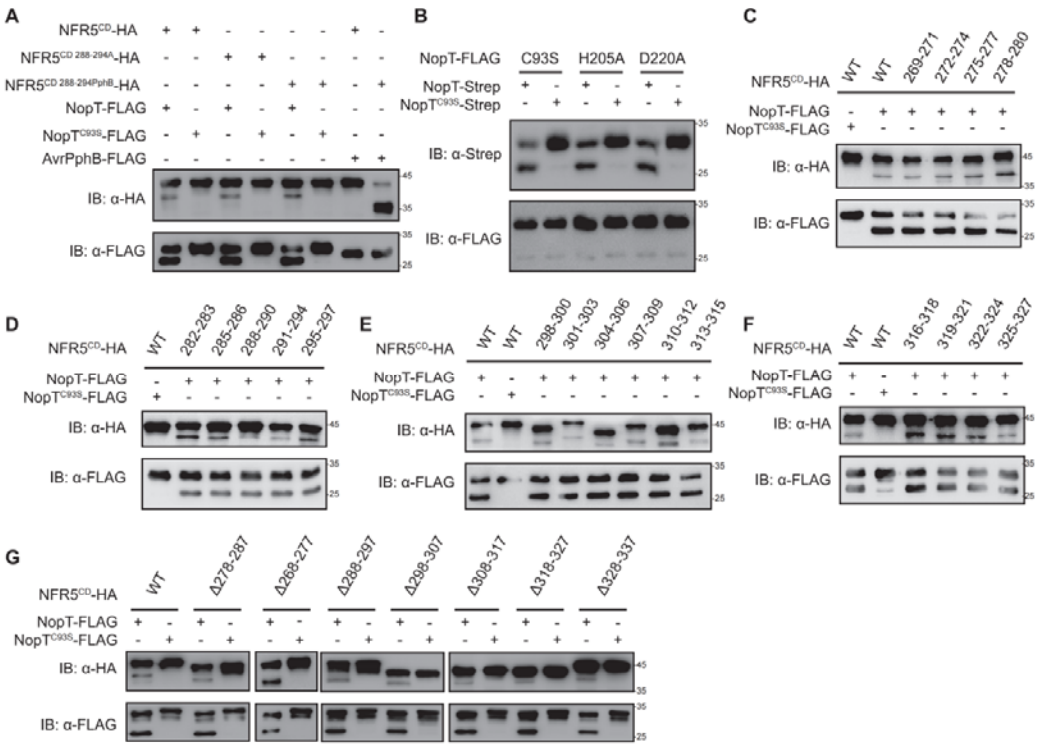

Supplemental Fig. 6. NopT cleaves NFR5 at the juxtamembrane domain.

(A) Cleavage assay using two mutant versions of $NFR5^{CD}$ in the presence of NopT or AvrPphB. $NFR5^{CD\ 288\text{-}294A}$ represents a mutant $NFR5^{CD}$ with residues 288 to 294 replaced with seven alanines; $NFR5^{CD\ 288\text{-}294PphB}$ represents a mutant $NFR5^{CD}$ with residues 288 to 294 replaced with AvrPphB recognition sites. (B) Autocleavage assay, using different NopT variants with single amino acid mutations. H205A and D220A indicate His-205 and Asp-220 replaced with alanine, respectively. (C-F) NopT cleavage assay using 19 variants of $NFR5^{CD}$ with three adjacent amino acids replaced with three alanines. The numbers indicate the location of the three residues replaced with alanines. (G) NopT cleavage assay using seven truncated variants of $NFR5^{CD}$ with 10 adjacent amino acids deleted. The numbers indicate the location of the 10 deleted residues.

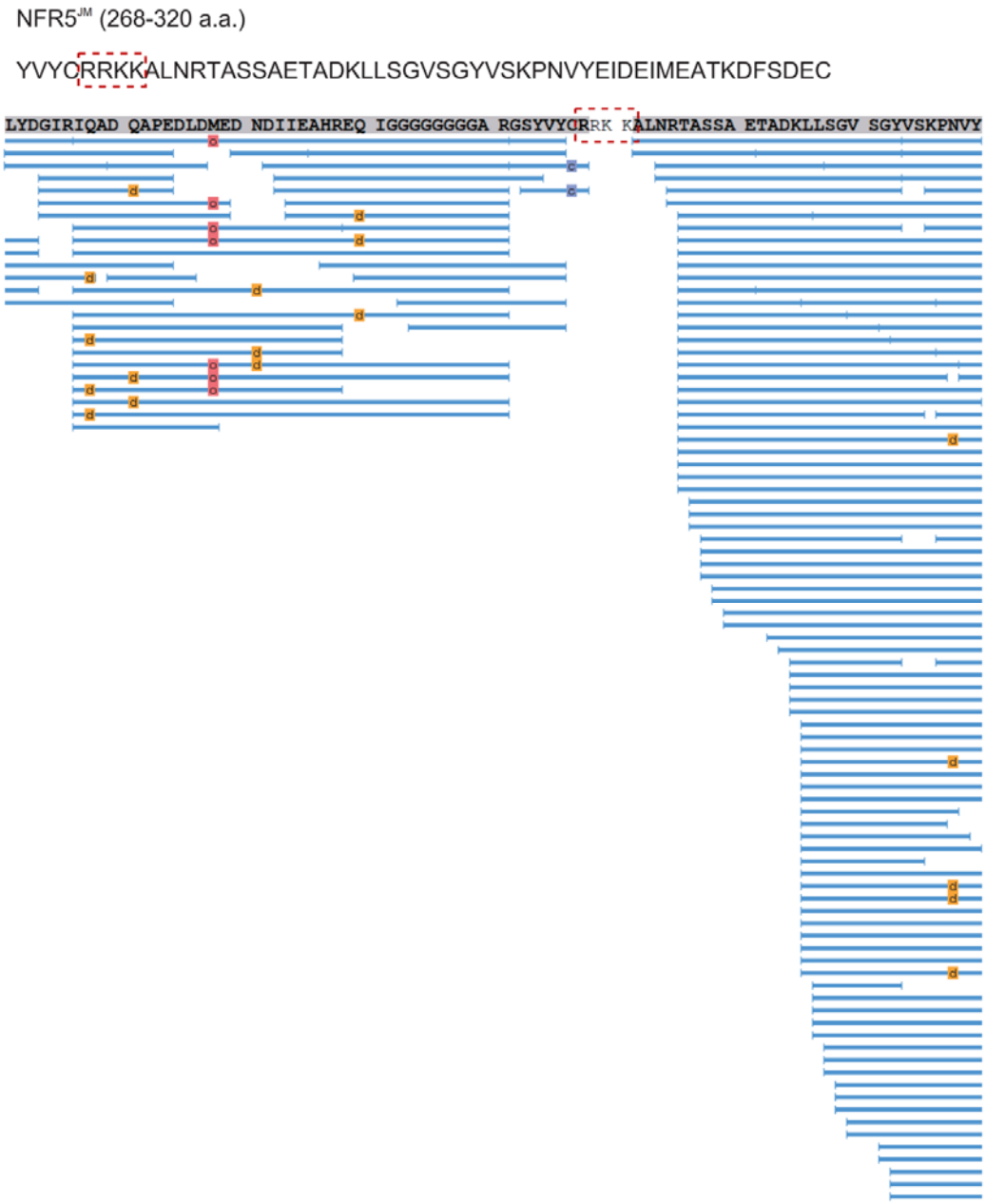

Supplemental Fig. 7. Mass spectrometry analysis of cleavage site of NFR5 by NopT.

(A) The sequence of NFR5 juxtamembrane domain (286-320 a.a.). (B) Mass spectrometry analysis of peptides of $NFR5^{CD}$ after proteolysis by NopT. Blue lines indicated the peptides characterized by Mass spectrometry. Red frame delineated cleavage site of NFR5 identified using Mass spectrometry.

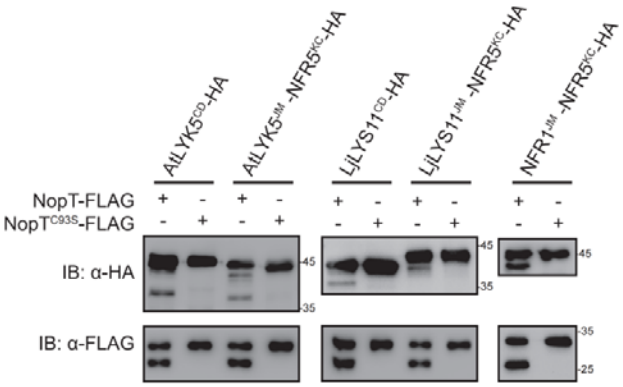

Supplemental Fig. 8. NopT cleaves the NFR5 homolog proteins at the juxtamembrane domain.

NopT but not NopT^{C93S} could cleave the CDs of AtLYK5 and LjLYS11 expressed in *E. coli*. NopT could cleave both AtLYK5^{JM}–NFR5^{KC}, LjLYS11^{JM}–NFR5^{KC} and NFR1^{JM}–NFR5^{KC}, three recombinant proteins expressed in *E. coli*. AtLYK5^{JM}–NFR5^{KC}, LjLYS11^{JM}–NFR5^{KC}, and NFR1^{JM}–NFR5^{KC} recombinant NFR5 proteins with the the JM was replaced with the JMs from AtLYK5, LjLYS11 and LjNFR1, respectively. KC: Kinase domain and C-terminal domain as ilustrated in Fig. S5A.

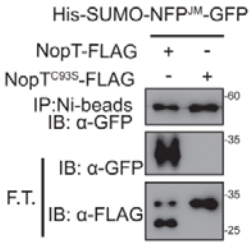

Supplemental Fig. 9. NopT cleaves the JM of MtNFP.

NopT cleaves a recombinant protein where His–tagged SUMO and GFP is bridged with the JM domain of NFP. F.T. represents flow through sample after Ni–beads purification. IB: immunoblotting.

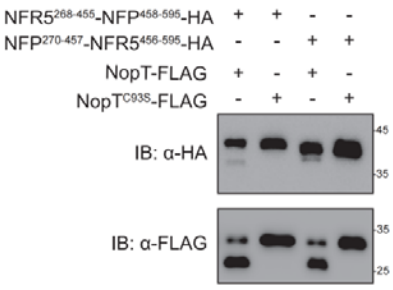

Supplemental Fig. 10. NopT cleaves recombinant proteins NFR5$^{268-445}$-NFP$^{458-595}$ and NFP$^{270-457}$-NFR$^{5456-595}$.

NopT but not NopT^{C93S} could cleave recombinant proteins NFR5$^{268-445}$-NFP$^{458-595}$ and NFP$^{270-457}$-NFR$^{5456-595}$ detected by immunobltting (IB).

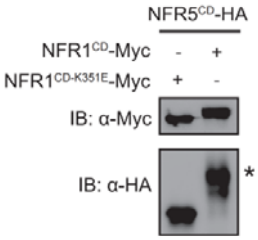

Supplemental Fig. 11. NFR1^{CD} phosphorylates NFR5^{CD} *in vitro*.

The cytoplasmic domains (CDs) of NFR1, NFR5, and kinase–dead NFR1$^{CD\text{-}K351E}$ were used for kinase assays in *E. coli*. Proteins were detected by immunoblotting using anti–HA and anti–Myc antibodies. Asterisk indicated the band retardation on the gel representing the phosphorylated NFR5^{CD} proteins.

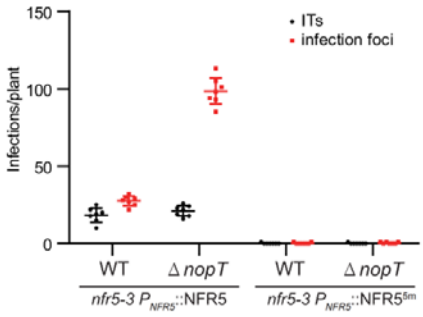

Supplemental Fig. 12. Rhizobial infection in the mutant versions of NFR5.

NFR5^{5m} failed to form rhizobial infection (n=7, Student's *t*–test: $P < 0.01$). The transgenic roots expressing NFR5 or NFR5^{5m} in the *nfr5-3* mutant under the control of native promoter were inoculated with GFP-labelled wild type NGR234 and NGR234Δ*nopT* respectively. The data was collected 9 days post inoculation. NFR5^{5m} represents a mutant version of NFR5 with S283Y, G294Q, Y304S, A310I, T311Y point mutation.

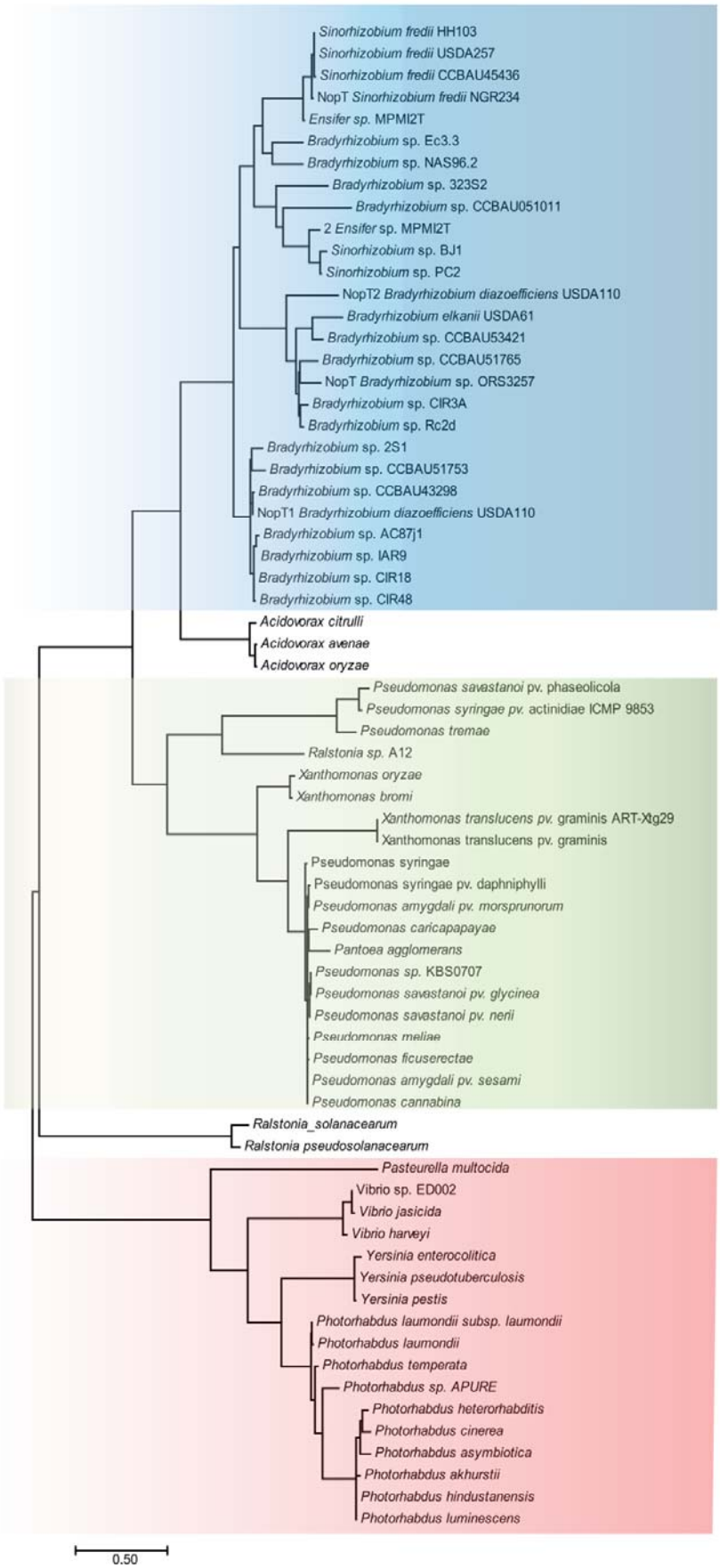
Sinorhizobium fredii HH103
Sinorhizobium fredii USDA257
Sinorhizobium fredii CCBAU45436
NopT Sinorhizobium fredii NGR234
Ensifer sp. MPMI2T
Bradyrhizobium sp. Ec3.3
Bradyrhizobium sp. NAS96.2
Bradyrhizobium sp. 323S2
Bradyrhizobium sp. CCBAU051011
2 Ensifer sp. MPMI2T
Sinorhizobium sp. BJ1
Sinorhizobium sp. PC2
NopT2 Bradyrhizobium diazoefficiens USDA110
Bradyrhizobium elkanii USDA61
Bradyrhizobium sp. CCBAU53421
Bradyrhizobium sp. CCBAU51765
NopT Bradyrhizobium sp. ORS3257
Bradyrhizobium sp. CIR3A
Bradyrhizobium sp. Rc2d
Bradyrhizobium sp. 2S1
Bradyrhizobium sp. CCBAU51753
Bradyrhizobium sp. CCBAU43298
NopT1 Bradyrhizobium diazoefficiens USDA110
Bradyrhizobium sp. AC87j1
Bradyrhizobium sp. IAR9
Bradyrhizobium sp. CIR18
Bradyrhizobium sp. CIR48
Acidovorax citrulli
Acidovorax avenae
Acidovorax oryzae
Pseudomonas savastanoi pv. phaseolicola
Pseudomonas syringae pv. actinidiae ICMP 9853
Pseudomonas tremae
Ralstonia sp. A12
Xanthomonas oryzae
Xanthomonas bromi
Xanthomonas translucens pv. graminis ART-Xtg29
Xanthomonas translucens pv. graminis
Pseudomonas syringae
Pseudomonas syringae pv. daphniphylli
Pseudomonas amygdali pv. morsprunorum
Pseudomonas caricapapayae
Pantoea agglomerans
Pseudomonas sp. KBS0707
Pseudomonas savastanoi pv. glycinea
Pseudomonas savastanoi pv. nerii
Pseudomonas meliae
Pseudomonas ficuserectae
Pseudomonas amygdali pv. sesami
Pseudomonas cannabina
Ralstonia_solanacearum
Ralstonia pseudosolanacearum
Pasteurella multocida
Vibrio sp. ED002
Vibrio jasicida
Vibrio harveyi
Yersinia enterocolitica
Yersinia pseudotuberculosis
Yersinia pestis
Photorhabdus laumondii subsp. laumondii
Photorhabdus laumondii
Photorhabdus temperata
Photorhabdus sp. APURE
Photorhabdus heterorhabditis
Photorhabdus cinerea
Photorhabdus asymbiotica
Photorhabdus akhurstii
Photorhabdus hindustanensis
Photorhabdus luminescens
0.50

Supplemental Fig. 13. Phylogenetic tree based on the amino acid sequence of NopT homologs from different bacterial species.

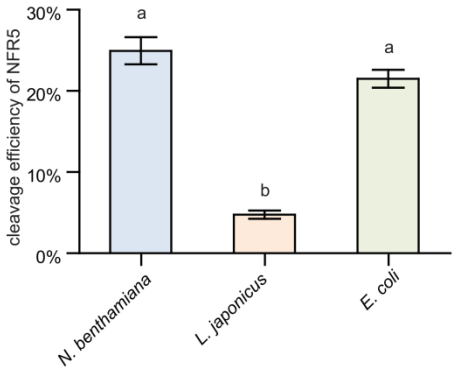

Supplemental Fig. 14. The cleavage efficiency of NFR5 in different system.

The relative cleavage efficiency for experiment displayed in Fig. 3A (*N. benthamiana*), Fig. 3B (*L. japonicus*) and Fig. 3D (*E. coli*) quantified from three biological replicates using ImageJ software. Values are means ± SE (n=3, Student t-test, letters represent significant differences, $p<0.05$).

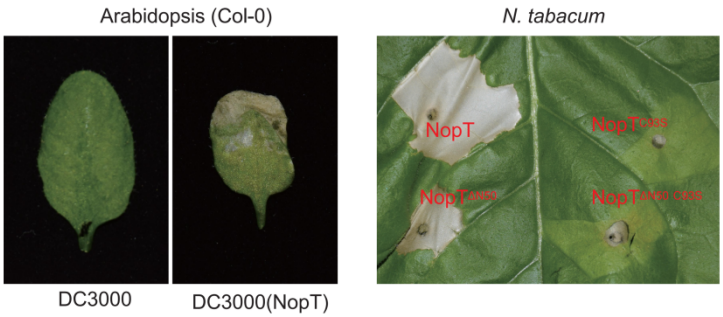

Supplemental Fig. 15. Transient expression of NopT triggers cell death in *Arabidopsis thaliana* and *Nicotiana tabacum*.

(A) *Pseudomonas syringae* pv tomato DC3000 harboring control plasmids (left) or expressing NopT (right) were infiltrated into Arabidopsis leaves. Pictures were taken three days post inoculation. (B) *Agrobacterium* strains harboring *NopT*, *NopT* with an N-terminal 50–amino acid deletion, $NopT^{C93S}$, or $NopT^{C93S}$ with an N-terminal 50–amino acid deletion were infiltrated into *N. tabacum* leaves. Pictures were taken three days post inoculation.

Supplemental Table 1. Phosphopeptides identified by liquid chromatography–mass spectrometry. An *in vitro* kinase assay was performed using the CD of NFR1 and NopT. NopT was separated by SDS-PAGE, and the digested gel slices representing the phosphorylated NopT were used for analysis. The deduced phosphopeptides are listed.

Sequence	Modifications	SITE	PSMs_NFR1$^{CD\text{-}KE}$+NopT	PSMs_NFR1+NopT
ETLANVELRTK	1xPhospho [T10]	37T	-	1
ETLANVELR	1xPhospho [T2]	29T	-	1
ETLANVELRTKSPSAECPDK	1xCarbamidomethyl [C17]; 1xPhospho [T10]	37T	-	1
TKSPSAECPDK	1xCarbamidomethyl [C8]; 1xPhospho [S5]	41S	-	1
SPSAECPDK	1xCarbamidomethyl [C6]; 1xPhospho [S3]	41S		1
SPSAECPDKMGCCASKPQASDPNNPSTSSPARPSTSLFR	3xCarbamidomethyl [C6; C12; C13]; 1xPhospho [S/T]; 1xOxidation [M10]		-	4
MGCCASKPQASDPNNPSTSSPARPSTSLFR	2xCarbamidomethyl [C3; C4]; 1xPhospho [T/S]; 1xOxidation [M1]		-	11
MGCCASKPQASDPNNPSTSSPARPSTSLFR	2xCarbamidomethyl [C3; C4]; 1xPhospho [T/S]		-	9
MGCCASKPQASDPNNPSTSSPARPSTSLFR	2xCarbamidomethyl [C3; C4]; 2xPhospho [T/S]	65S 66T	-	4
MGCCASKPQASDPNNPSTSSPARPSTSLFR	2xCarbamidomethyl [C3; C4]; 1xOxidation [M1]		4	2
MGCCASKPQASDPNNPSTSSPARPSTSLFR	2xCarbamidomethyl [C3; C4]; 2xPhospho [T/S]; 1xOxidation [M1]		-	4
TAELAQANADGICVGLTAEWLR	1xCarbamidomethyl [C13]; 1xPhospho [T17]	97T	-	10
NLNSHPSIR	1xPhospho [S7]	109S	-	2
NLNSHPSIRMEALVPGSQR	1xPhospho [S7]; 1xOxidation [M10]	119S	-	1
MEALVPGSQR	1xPhospho [S8]	119S	-	1
MEALVPGSQR	1xPhospho [S8]; 1xOxidation [M1]	119S	-	1
RQGAGPSEADFAAQNTMLQK	1xPhospho [T/S]; 1xOxidation [M17]		-	3
RQGAGPSEADFAAQNTMLQK	1xPhospho [T16]	156T	-	2
QGAGPSEADFAAQNTMLQK	1xPhospho [T/S]; 1xOxidation [M16]		-	3
QGAGPSEADFAAQNTMLQK	1xPhospho [T15]	156T	-	2
SLANRYSNPNR	1xPhospho [S7]	245S	-	2
QHLTTVTTQK	1xPhospho [T8]	257T	-	1

1452 **Supplemental Table 2. Primers used in this study.**

Used for	Target genes	Names	Sequences (from 5' to 3')
Overexpression in Nicotiana benthamiana	NopT or NopT^{C93S}	p5X-NopT-F	agaacacgggggactctagaatgcacagtcccatcag
		p5X-NopT-R	ccgctgttatcggtacctgtcatcttttgggtggtcac
	NopT$^{\Delta N50}$	p5X-NopTdeN50-F	agaacacgggggactctagaatgtgctgcgccagcaag
	NFR1	p5X-NFR1-F	agaacacgggggactctagaatgaagctaaaaactggtctact
		p5X-NFR1-R	ccgctgttatcggtacctcttctcacagac
	NFR5	p5X-NFR5-F	agaacacgggggactctagaatggctgtcttctttcttacc
		p5X-NFR5-R	ccgctgttatcggtaccacgtgcagtaat
		p5X-NFR5gfp-R	tcccgggagcggtaccacgtgcagtaatggaagt
	AvrPphB	p5X-AvrPphB-F	agaacacgggggactctagaatgaaaataggtacgcaggcc
		p5X-AvrPphB-R	ccgctgttatcggtacccgaaactctaaactcgtttacgc
templates for protein expression	NopT$_{USDA257}$	p5X-257T-F	agaacacgggggactctagatgctgcgtgatccgaacaat
		p5X-257T-R	ccgctgttatcggtacctgtcacctttgggtggtcaccg
	NopT1$_{USDA110}$	p5X-110T1-F	agaacacgggggactctagaatgtatgatcgaatcggtgg
		p5X-110T1-R	ccgctgttatcggtaccctgcatcctttgcgtcg
	NopT2$_{USDA110}$	p5X-110T2-F	agaacacgggggactctagaatgtataatcgagtcgatggc
		p5X-110T2-R	ccgctgttatcggtaccccgatgaggttccgc
Protein Expression in *E.coli*	NopT or NopT^{C93S}	28a NopT-F	tgggtcgcggatccgaattcatgcacagtcccatcag
		28a FLAG-R	tcgagtgcggccgcaagcttcttgtcatcgtcatccttgtag
		28a Strep-R	tcgagtgcggccgcaagctttttttcaaattgaggatgagaccatcc
	AvrPphB	ET28a-pphb-F	tgggtcgcggatccgaattcaaaataggtacgcaggccac
	NopT$_{USDA257}$	ET28a-257T-F	tgggtcgcggatccgaattcctgcgtgatccgaacaa
	NopT1$_{USDA110}$	ET28a-110T1-F	tgggtcgcggatccgaattctatgatcgaatcggtggctc
	NopT2$_{USDA110}$	ET28a-110T2-F	tgggtcgcggatccgaattctataatcgagtcgatggcgaatac
	NFR1^{CD}	duet NFR1-F	accacagccaggatccgagataccagaagaaggaagaagagaaagc
		duet Sac1nost-R	ggcgcgccgagctcgcgatcggggaaattcgagct
	NFR5^{CD}	ACSH-NFR5-F	agaagcgcggatccgaattctatgtatactgccgcagaaagaag
		ACSH-NFR5-R	cgtatgggtagcttccaagcttacgtgcagtaatggaagtc
	NFR5^{KD}	SUMO 5KD-F	ccgcgaacagattggtaaggttggggaatcagtgtac
		SUMO HA-R	gctcgaattcggatcctttcacgcatagtcaggaacatcg
	NFR5^{JM}	SUMO 5JM-F	ccgcgaacagattggttatgtatactgccgcagaaagaag
		SUMO 5JM-R	gctcgaattcggatcctttcacgcatagtcaggaacatcg
	sumo-NFR5^{KD}-HA	duet sumo-F	catcaccacagccaggatgggtccctgcaggac
		duet HA-R	cattatgcggccgcaagcttttacgcatagtcaggaacatcg
	sumo-NFR5^{JM}-GFP	duet sumo-F	catcaccacagccaggatgggtccctgcaggac
		duet GFP-R	atgcggccgcaagcttttacttgtacaactcatccatacc

	AtLYK5	ACSH-LYK5-F	gcgcggatccgaattctacaaacgaaggtctaagaag
		ACSH-LYK5-R	ggtagcttccaagcttgttgccaagagagccg
	LjLYS11	ACSH-LYS11-F	agaagcgcggatccgaattcacttgtctgaggaagagaaag
		ACSH-LYS11-R	cgtatgggtagcttccaagcttacgagctgctatcaaagtt
	$LYK5^{JM}$ $NFR5^{KD}$	LYK5-NFR5-F	cgaaaacagaaaggttggggaatcagtg
		NFR5 LYK5-R	ccccaacctttctgttttcgtcgctgaaatt
	$LYS11^{JM}$ NFR5KD	LYS11 NFR5-F	gagcagtgtaaggttggggaatcag
		NFR5 LYS11R	ccccaaccttacactgctcattgagg
	NFP^{JM}	ACSUG NFPJ-F	gtggaggcgctagaggatcctattgtctcaaaatgaagagattgaatagaag
		ACSUG NFPJ-R	cttctcccttagagagctcacaattgtcactcagattcattg
	$NFR5^{JM}$-NFP^{KD}	5JM-PKD-F	gatgagtgcaagattggtgaatcagtttacaaag
		5JM-PKD-R	accaatcttgcactcatcgct
	NFP^{JM}-$NFR5^{KD}$	PJM-5KD-F	gacaattgtaaggttggggaatcagtg
		PJM-5KD-R	ccccaaccttacaattgtcactcagattcattg
	$NFR5^{268-445}$-$NFP^{458-595}$	51/2KD-P1/2KD-F	ccatggccagaacttcaaccaactcaat
		51/2KD-P1/2KD-R	gaagttctggccatggcgaa
	$NFP^{270-457}$-$NFR^{5456-595}$	P1/2KD-51/2KD-F	ggatggctagaacttcgaccaac
		P1/2KD-51/2KD-R	cgaagttctagccatcccgaa
site mutantions construction	NopT	T93S-F	gaatctccgtcggcttgactgc
		T93S-F	gacggagattccatctgcgttc
		97D-F	ggcttggatgcggagtggctgcg
		97D-R	ctccgcatccaagccgacgcag
		97A-F	ggcttggctgcggagtggctgc
		97A-R	ctccgcagccaagccgacg
		109D-F	catccggatatccgaatggaggccctag
		109D-R	ttcggatatccggatgactgttgaggttacgc
		109A-F	catccggcaatccgaatggag
		109A-R	ttcggattgccggatgactgttg
		119D-R	cccggagatcaaaggcacgcctcagc
		119A-F	gcctttgatctccgggtactagggcc
		119A-F	cccggagcgcaaaggcac
		119A-R	ctttgcgctccgggtactagg
		156D-F	gcaaaacgatatgttgcagaaagcaggc
		156D-R	gcaacatatcgttttgcgccgcgaagtcggcc
		156A-F	gcaaaacgctatgttgcagaaagcag
		156A-R	ctgcaacatagcgttttgcgccgcgaagtc
		H205A-F	ggcggcaacaccgttgcgacc
		H205A-R	caacggtgttgccgccgccctcagc
		D220A-F	ctcttcgctcctaatttcggcgaatttac
		D220A-R	gccgaaattaggagcgaagagcgtggtgtttc

		245D-F	cgctacgacaatccaaaccggcag
		245D-R	ttggattgtcgtagcgattggctaggct
		257 mutants	changing the sequence of r primer at noptt257when cloned into vectors
	NFR1	K351E-F	gcaattgagaagatggatgtacaagcatc
		K351E-R	catccatcttctcaattgctgttttcttgcc
	NFR5	269-271A-F	ctatgcagctgcacgcagaaagaaggctctg
		269-271A-R	gcgtgcagctgcatagaattcggatccgcgc
		272-274A-F	ctgcgctgcagctaaggctctgaataggactgc
		272-274A-R	cttagctgcagcgcagtatacatagaattcggatcc
		275-277A-F	gaaaggcagctgcaaataggactgcttcatcagc
		275-277A-R	ctatttgcagctgcctttctgcggcagtatacatag
		278-280A-F	ctggctgcagctgcttcatcagctgagactg
		278-280A-R	agcagctgcagccagagccttctttctgcg
		282-283A-F	gcagcagctgagactgctgataaactac
		282-283A-R	gcagtctcagctgctgcagcagtcctattcagag
		285-286A-F	ggggctgctgataaactactttctggag
		285-286A-R	agtagtttatcagcagccccagctgatgaagcagtc
		288-290A-F	gctgcagcactttctggagtttcaggctatgtaag
		288-290A-R	aaactccagaaagtgctgcagcagcagtctcagctgatgaag
		291-294A-F	gagactgctgataaactagctgctgcagtttcaggctatgtaagcaagcc
		291-294A-R	atagcctgaaactgcagcagctagtttatcagcagtctcagctg
		295-298A-F	gagttgcagctgctgtaagcaagccaaacgtgtatg
		295-298A-R	cttacagcagctgcaactccagaaagtagtttatcagcag
		298-300A-F	ctatgcagctgcaccaaacgtgtatgaaatcgacg
		298-300A-R	gtttggtgcagctgcatagcctgaaactccagaaagtag
		301-303A-F	gcaaggcagctgcttatgaaatcgacgagataatggaagc
		301-303A-R	cataagcagctgccttgcttacatagcctgaaactcc
		304-306A-F	gtggctgcagctgacgagataatggaagctacgaag
		304-306A-R	cgtcagctgcagccacgtttggcttgcttacatagc
		307-309A-F	gaaatcgctgcagcaatggaagctacgaaggatttcag
		307-309A-R	ccattgctgcagcgatttcatacacgtttggcttgc
		310-312A-F	cgagatagcagctgctacgaaggatttcagcg
		310-312A-R	gtagcagctgctatctcgtcgatttcatacacgtttg
		313-315A-F	gctgcagctgcattcagcgatgagtgcaagg
		313-315A-R	ctgaatgcagctgcagcttccattatctcgtcgatttc
		316-318A-F	ggatgcagctgctgagtgcaaggttggggaatc
		316-318A-R	ctcagcagctgcatccttcgtagcttccattatctc
		319-321A-F	cgatgctgcagctgttggggaatcagtgtacaagg
		319-321A-R	caacagctgcagcatcgctgaaatccttcgtagc

		322-324A-F	gcaaggcagctgcatcagtgtacaaggccaacatag
		322-324A-R	gatgcagctgccttgcactcatcgctgaaatc
		325-327A-F	gaagcagctgcaaaggccaacatagaaggtcg
		325-327A-R	gcctttgcagctgcttccccaaccttgcactc
		268-277DE-F	agaagcgcggatccgaattcaataggactgct
		268-277DE-R	ctgatgaagcagtcctattgaattcggatccgcgcttc
		278-287DE-F	gcagaaagaaggctctggataaactactttctggagtttcagg
		278-287DE-R	aaactccagaaagtagtttatccagagccttctttctgcg
		298-307DE-F	caggctatgagataatggaagctacgaaggatttc
		298-307DE-R	cttccattatctcatagcctgaaactccagaaagtag
		308-317DE-F	gaaatcgacgatgagtgcaaggttgggg
		308-317DE-R	ttgcactcatcgtcgatttcatacacgtttggc
		318-327DE-F	gatttcagcaaggccaacatagaaggtcg
		318-327DE-R	gttggccttgctgaaatccttcgtagcttcc
		328-337DE-F	tcagtgtacgtaaagaaaatcaaggaaggtggtgcc
		328-337DE-R	attttctttacgtacactgattccccaaccttg
		288-294A-F	gcagctgccgcagcggctgcctcaggctatgtaagcaagcc
		288-294A-R	gcagccgctgcggcagctgcagcagtctcagctgatgaagc
		288-298PBS1-F	ggagacaaatctcatgtctcctcaggctatgtaagcaagcc
		288-298PBS1-R	ggagacatgagatttgtctccagcagtctcagctgatgaagc
		N5-283S-R	tgaagcagtcctattcagagcc
		283Y-F	tctgaataggactgcttcatacgctgagactgc
		N5-294G	agaaagtagtttatcagcagtctcag
		294Q-F	ctgctgataaactactttctcaggtttcaggctatgtaag
		N5-303Y-R	cacgtttggcttgcttacatag
		304S-F	gcaagccaaacgtgtccgaaatcgacgag
		N5-310AT-R	ttccattatctcgtcgatttcatacac
		311-2 IY-F	gaaatcgacgagataatggaaatctacaaggatttcagcgatgagtg
Complem ental	NopT	HC-proT-F	gaattcgagctcggtacctcatggccttccttggagg
		T-3-F	cacagtcccatcagtggttc
		T-3-R	gaaccactgatgggactgtg
		HC-T-R	cgcgggatcgagatctcgagtcatgtcatcttttgggtggtc
	NFR5	cherry-proNFR5-F	ccaagctgggctgcagggacatgagattgaagctcc
		proNFR5-NFR5-F	ccccacttcacaaacatggctgtcttctttcttacctc
		proNFR5-NFR5-R	gccatgtttgtgaagtgggg
		NFR5-JM-KD-F	gatgagtgcaaggttgggg
		NFR5-JM-KD-R	ccccaaccttgcactcatc
		cherry kpn1	
		Sac1-R	ggcgcgcctaggtaccggggaaattcgagc

1453